Early to Late Pleistocene history of debris-flow fan evolution in western Death Valley using cosmogenic ^{10}Be and ^{26}Al

Miriam Dühnforth[1*], Alexander L. Densmore[2], Susan Ivy-Ochs[3], Philip Allen[4], Peter W. Kubik[3]

[1] Department of Earth and Environmental Science, LMU Munich, Germany
[2] Institute of Hazard and Risk Research and Department of Geography, Durham University, Durham, UK
[3] Laboratory of Ion Beam Physics, ETH Zurich, Switzerland
[4] Department of Earth Science and Engineering, Imperial College, London, UK

*corresponding author:
phone +49 89 2180 6714, email miriam.duehnforth@lmu.de

Keywords: debris-flow fan; cosmogenic dating; Death Valley; inheritance

Highlights

- Debris-flow fans on the western side of Death Valley preserve a long depositional chronology with early to late Pleistocene surface dates
- ^{10}Be and ^{26}Al measurements show continuous exposure history on the fan
- Inheritance complicates interpretation of the true depositional ages
- Surface smoothing with elimination of debris-flow morphology takes a few 10^5 ka

Abstract

Debris-flow fans with depositional records over several 10^5 years may be useful archives for the understanding of fan construction by debris flows and post-depositional surface modification over long timescales. Reading these archives, however, requires that we establish the temporal and spatial pattern of debris-flow activity over time. We used a combination of geomorphic mapping of fan surface characteristics, digital topographic analysis, and cosmogenic radionuclide dating using ^{10}Be and ^{26}Al to study the fan evolution of the Warm Springs fan on the west side of southern Death Valley, California. The ^{10}Be concentrations yield dates that vary from 989 ± 43 to 595 ± 17 ka on the proximal fan and between 369 ± 13 and 125 ± 5 ka on distal fan surfaces. The interpretation of these results as true depositional ages though is complicated by high inheritance with a minimum of 65 ka measured at the catchment outlet and of at least 125 ka at the distal fan. Results from the ^{26}Al measurements suggest that most sample locations on the fan surfaces underwent simple exposure and were not affected by complex histories of burial and re-exposure. This implies that Warm Springs fan is a relatively stable landform that underwent several 10^5 years of fan aggradation before fan head incision caused abandonment of the proximal and central fan surfaces and deposition continued on a younger unit at the distal fan. We show that the primary depositional debris-flow morphology is eliminated over a time scale of less than 10^5 years, which prevents the delineation of individual debris flows as well as the precise reconstruction of lateral shifts in deposition as we find it on younger debris-flow fans. Secondary post-depositional processes control subsequent evolution of surface morphology with the dissection of planar surfaces while smoothing of convex-up interfluves between incised channels continues through time.

1. Introduction

Debris-flow fans are depositional landforms that record the history of sediment transfer from the source area to the sedimentary sink on the fan. In coupled catchment-fan systems along mountain fronts, the production of sediment in the catchment, the occurrence of debris flows, and the subsequent deposition of sediment on the fan are modulated by a variety of different controls. These include tectonic, climatic, and internal mechanisms as well as changes in base level. Over time repeated debris-flow activity results in a distinct spatial and temporal pattern of sediment deposition on the fan (e.g. Bull, 1964; Bull, 1977; Gordon and Heller, 1993; Whipple and Trayler, 1996). Assessing these sediment records allows us to understand the history of fan construction and how debris-flow fan surfaces evolve through time.

One first-order boundary condition for the evolution of a sediment fan and its geometry is set by the pattern and rate of basin subsidence, which controls the amount of sediment accommodation and hence the thickness and spatial extent of the fan (Gordon and Heller, 1993; Whipple and Trayler, 1996). On debris-flow fans, debris-flows migrate across the fan surface by lateral and radial shifts in deposition. Lateral shifts result from avulsion of individual flows (Hooke, 1967; Whipple and Dunne, 1992), which over time can lead to resurfacing of a whole alluvial fan. Radial shifts in the depocenter can either occur as backstepping or basinward migration of the depocenter. The latter is often caused by fan head incision, initiated by base level lowering, changes in the sediment transport capacity of the alluvial fan system, or autogenic processes (e.g., Harvey, 2002; Kim and Jerolmack, 2007; Nicholas and Quine, 2007; Dühnforth et al., 2008; Clarke et al., 2010), and leads to abandonment and preservation of older fan units. Both, lateral and radial changes in the depocenter, result in the construction of a debris-flow fan

97 characterized by multiple individual surface units, each of which was active at a different time
98 (Denny, 1965; Hooke, 1967; Wells et al., 1987; Blair and McPherson, 1994; Ritter et al., 2000;
99 Dühnforth et al., 2007; Harvey, 2011; Ventra and Nichols, 2014; d'Arcy et al., 2015). Cross-
100 cutting relationships between individual debris-flow channels and levees as well as differences in
101 the degree of weathering of debris-flow boulders are useful criteria to identify individual fan
102 surface units (Whipple and Dunne, 1992; Dühnforth et al., 2007; Le et al., 2007; Schürch et al.,
103 2016). The history of fan occupation in time and space including the migration of the sediment
104 depocenter can therefore be reconstructed by using the morphological properties on the fan
105 surfaces in combination with numeric dating techniques (Bierman et al., 1995; Zehfuss et al.,
106 2001; Dühnforth et al., 2007; Le et al., 2007; Schürch et al., 2016). While many studies on
107 debris-flow fan activity have established fan chronologies with ages younger than 100 ka, it is
108 not clear how far back in time we can reconstruct debris-flow fan activity as previous results
109 have shown that primary depositional morphology becomes obscured or removed by secondary
110 processes over time (e.g., Wells et al., 1987; Bull, 1991; Matmon et al., 2006; Frankel and
111 Dolan, 2007; Regmi et al., 2014). Models of fan surface relief evolution suggest that the
112 degradation of the original depositional morphology leads to smoothing of alluvial fan surfaces
113 after abandonment. With ongoing time these smooth surfaces become dissected by channels with
114 an increase in the relief between channel floors and interfluves (Wells et al., 1987; Bull, 1991;
115 Matmon et al., 2006; Frankel and Dolan, 2007; Regmi et al., 2014). It would therefore be useful
116 to estimate the age range over which a fan surface preserves a record of debris-flow deposition,
117 which in turn requires analysis of fans with chronologies that extend back for several 10^5 years.
118 This time scale is long enough to examine the long-term evolution of a debris-flow fan without
119 the inherent variability in the tectonic and climatic boundary conditions. So far only a limited

number of field studies are available that address the pattern of debris-flow deposition in combination with numeric age constraints to explore the long-term signal of debris flow activity preserved on the alluvial fan.

Arid-region alluvial fans in the southwestern United States are a well-studied target for sedimentary processes on alluvial fans and have a good record of numeric age control. Results from numeric dating techniques such as cosmogenic ^{10}Be and ^{26}Al dating, ^{14}C dating, Optical Stimulated Luminescence (OSL), or tephronochronology show that the majority of alluvial fan surfaces in the southwest of North America have ages younger than 100 ka (Owen et al., 2014 and references therein). Only a limited number of alluvial fans in the southwestern United States show dates close to or older than 10^5 years (e.g. Bierman et al., 1995; Reheis et al., 1996; Matmon et al., 2005; Matmon et al., 2006; Frankel et al., 2007a; Frankel et al., 2007b; Machette et al., 2008; Spelz et al., 2008; Owen et al., 2011; Gray et al., 2014; Owen et al., 2014). Debris-flow dominated fans on the west side of southern Death Valley show exceptionally old surfaces with dates extending back to around 400 ka (Nishiizumi et al., 1993; Liu and Broecker, 2008; Machette et al., 2008). Therefore, these debris-flow fans represent ideal targets to study the long-term dynamics of debris-flow fan activity and surface modification over a period that includes multiple 10^5 years. We aim to build upon the existing dataset of numeric alluvial fan chronologies in the Death Valley/Mojave Desert region and use these time constraints as reference for a comprehensive study of numeric ages across an individual fan in Death Valley. A relatively dense pattern of multiple sampling sites across an entire fan would allow the construction of a numeric age chronology that records times and durations of fan activity and abandonment. The chronology also enables us to assess the time scale over which post-

143 depositional change of the fan surfaces occur. Both, the timing on fan deposition and post-
144 depositional modification of fan surfaces allows us to validate the time scale over which existing
145 models of fan evolution with surface smoothing and dissection operate.
146
147 The strategy is first to establish a relative age chronology of fan deposition, which in turn guides
148 our sampling for a numeric age chronology using cosmogenic ^{10}Be and ^{26}Al. Especially on
149 depositional surfaces with ages older than several 10^5 years, the influence of surface erosion or
150 surface reworking may limit our ability to measure true depositional ages. In addition, the
151 amount of inheritance can make up a significant fraction of the total nuclide concentration in a
152 sample, which challenges the interpretation as depositional age (Anderson et al., 1996; Hancock
153 et al., 1999). Therefore, the amount of inheritance will have to be determined, as inheritance on
154 alluvial fans in Death Valley can be up to 100 ka (Machette et al., 2008; Owen et al., 2011;
155 Frankel et al., 2015). Based on a combination of field work, analysis of digital airborne swath
156 mapping (ALSM) topographic data, and cosmogenic surface exposure dating using in-situ ^{10}Be
157 and ^{26}Al, our goal is (a) to establish a relative and numeric age chronology on an individual
158 alluvial fan, (b) to investigate the temporal and spatial pattern of numeric age constraints, and c)
159 to evaluate the time scale over which primary debris-flow morphology is removed by post-
160 depositional fan surface modification.
161
162 **2. Setting**
163 We focus on the Warm Springs fan located on the western side of Death Valley in the
164 southwestern United States (Fig. 1). Death Valley is an extensional half-graben bounded on its
165 eastern margin by the oblique-normal Black Mountain fault zone (BMFZ). To the north and

166 south, the BMFZ merges with the right-lateral Northern Death Valley fault zone (NDVFZ) and
167 Southern Death Valley fault zone, respectively (Machette, 2001). The slip rate of the NDVFZ is
168 approximately 4-5 mm yr^{-1} averaged over the past 100 ka (Frankel et al., 2007b). For the BMFZ,
169 the minimum normal slip rate calculated over that past 120-186 ka is 0.15-0.2 mm yr^{-1} (Knott
170 and Wells, 2001), while Holocene vertical slip rates have been estimated at 1-3 mm/yr (Klinger
171 and Piety, 2001) and 0.5-2 mm/yr (Frankel et al., 2015). Minor normal faulting also occurs along
172 the western margin of Death Valley on the West Side Fault Zone (Machette et al., 2008). Normal
173 slip on the BMFZ leads to large accommodation on the east side of the valley, and less
174 accommodation on the west side (Hooke, 1972), so that fan deposits on the western side are
175 generally thinner but larger in surface area (~20-40 km^2) than those on the east, with long radial
176 lengths from apex to toe (e.g. Hunt and Mabey, 1966; Hooke, 1972; Gordon and Heller, 1993;
177 Whipple and Trayler, 1996). As the rate of resurfacing is high on the eastern alluvial fans in
178 Death Valley, these alluvial fans show younger age chronologies compared to fan surfaces on the
179 west side (Machette et al., 2008; Owen et al., 2011; Frankel et al., 2015).
180 The Warm Springs fan, in the southwestern corner of the basin, stands out from all other debris-
181 flow fans on the west side of southern Death Valley with its prominent surface relief, expressed
182 as the elevation difference between interfluves and incised channel floors (Fig. 1). Therefore, the
183 Warm Springs fan is well-suited to test models of post-depositional surface evolution (Matmon
184 et al., 2006; Frankel and Dolan, 2007; Regmi et al, 2014). Based on such model we expect to
185 find the oldest surface dates at the proximal fan, where the relief between channel floors and
186 interfluves is highest while undissected distal fan areas would be younger.
187 The Warm Springs fan is sourced in the Panamint Range and has a surface area of about 30 km^2
188 (Fig. 1). The topographic elevation of the fan varies from about 60 m below sea level at the distal

189 fan margin to about 360 m above sea level at the fan head. Several NNE-SSW-trending antithetic
190 and synthetic normal faults of the West Side Fault Zone run across the fan (Hooke, 1972; Blair,
191 1999a), with fault scarp heights that range between a few meters to several tens of meters. Blair
192 (1999a) pointed out that this local faulting pattern strongly controls sedimentation and surface
193 preservation on the Warm Springs fan. Sediment is supplied to the fan by debris flows
194 originating in the associated Warm Springs catchment, as shown by the fan stratigraphy (Blair
195 1999a; Blair, 1999b). Sediment is stored in small alluvial cones in the catchment area, and these
196 cones are the sediment source for debris flows exiting onto the Warm Springs fan. The debris
197 flows contain cobbles and boulders of Precambrian to Paleozoic quartzite, dolomite, and shale,
198 Mesozoic granite, and Triassic to Jurassic andesite (Johnson, 1957; Jennings et al., 1962; Miller,
199 1985). Debris-flow deposits exposed in incised channel walls on the alluvial fan are commonly
200 preserved as meter-thick, matrix-rich units with abundant cobble-sized clasts (2-30 cm) and low
201 to moderate concentrations of boulders with sizes up to 1 to 2 m.

202 As with other debris-flow fans on the western side of Death Valley, the Warm Springs fan
203 head is incised by an active channel, in this case about 30 m deep and 300 m wide (Fig. 2). The
204 incision resulted in a basinward shift of the active depocenter to the distal part of the fan, and has
205 been attributed to tectonic activity and eastward tilting of the fan surface (Hunt and Mabey,
206 1966; Hooke, 1972; Hooke and Dorn, 1992). Older depositional surfaces on the fan are also
207 dissected by channel incision, resulting in the formation of elongated ridges (Fig. 2). Interfluves
208 are generally planar with very low cross-sectional curvature, except where channel spacing is
209 narrow and diffusional channel margins have coalesced into gently-curved, convex-upwards
210 ridge crests. These planar interfluve surfaces often have well-developed desert pavements
211 composed of closely-interlocking, varnished clasts of sizes similar to those found in the channel

212 walls (Fig. 3). Boulders are rare on both proximal and medial fan surfaces, but are relatively
213 frequent in the incised channels and in the more recent deposits at the distal fan.
214
215 While the present-day climate in Death Valley is extremely arid, with an annual mean
216 precipitation rate of less than 65 mm yr^{-1} (Western Region Climate Center –
217 http://www.wrcc.dri.edu), paleoclimatic studies from Death Valley and adjacent basins have
218 documented significant hydrologic variations since 1.2 Ma (Smith, 1984; Winograd et al., 1985;
219 Jannick et al., 1991; Smith and Bischoff, 1997; Lowenstein et al., 1999). Evidence for large
220 paleolakes, indicating generally wetter climate conditions, has been found in sediments from
221 Searles, Panamint, Owens, and Death Valley basins (Smith, 1984; Jannick et al., 1991; Li et al.,
222 1996; Ku et al., 1998; Lowenstein et al., 1999; Forester et al., 2005). In Death Valley, the
223 Badwater sediment core combined with outcrop dates provide direct evidence for a large lake
224 between 186 and 120 ka and a smaller lake between 35 and 10 ka (Ku et al., 1998; Lowenstein et
225 al., 1999). According to micropalaeontologic data (Forester et al., 2005), the highest lake level in
226 the past 200 ka occurred at ~155 ka. Machette et al. (2008) determined that the Lake Manly lake
227 level was at 30 m a.s.l. at 130 ka, and noted that higher shoreline deposits on the Hanaupah
228 Canyon fan at >67 m a.s.l. may be related to a lake level highstand during marine isotope stage
229 (MIS) 6 or possibly MIS 8. On the Warm Springs fan, a paleoshoreline is cut into the distal fan
230 deposits at a topographic elevation of ~65 m a.s.l. (Hooke, 1972; Blair, 1999b) (Fig. 2). It is very
231 likely that this shoreline is related to the lake level highstand during MIS 6 (Hooke and Dorn,
232 1992; Blair, 1999a; Knott et al., 2002; Machette et al., 2008; Owen et al., 2011).
233
234

3. Prior fan surface chronologies in Death Valley

Debris-flow fans on the western side of Death Valley have been the subject of numerous investigations of depositional processes and surface evolution on arid-region fans (e.g. Denny, 1965; Hunt and Mabey, 1966; Hooke, 1972; Hooke and Dorn, 1992; Blair, 1999b). Many of these studies have mapped different depositional units and established a relative fan chronology. Denny (1965) and Hunt & Mabey (1966) were the first to publish a relative age chronology for alluvial fan surfaces in Death Valley based on stratigraphic relationships, soil development, the degree of desert pavement and rock varnish development, and the distribution of boulder sizes, and this approach has since been widely applied to other alluvial surfaces beyond Death Valley (e.g. Bull, 1991).

On the Warm Springs fan, Hunt and Mabey (1966) mapped three different alluvial fan units, termed Qg2, Qg3, and Qg4 in order of decreasing age. We note that Hunt and Mabey (1966) also described an even older alluvial fan unit QgT1 (Q1 according to Knott et al., 2005), which was characterized as a degraded form of surface unit Qg2 showing a lack of desert pavement and rock varnish (Menges et al., 2001) or only patches of well-developed desert pavement (Hooke, 1972). Even though this unit has not been identified on the Warm Springs fan (Hunt and Mabey, 1966), this older unit has been mapped for example on the Hanaupah Canyon fan (Fig. 1) (Hooke, 1972; Menges et al., 2001). According to Hunt and Mabey (1966) deposits of unit Qg2 generally form the highest surfaces above the present-day washes. They are characterized by well-developed, smooth desert pavement of highly varnished clasts underlain by a several-centimeter thick Av-horizon consisting mainly of eolian silt and clay. Underneath the Av-horizon, cementation of clasts by calcium carbonate (caliche) is ubiquitous. Unit Qg3 is located more towards the toe of the Warm Springs fan and overlaps unit Qg2 at its lowest position (Hunt

and Mabey, 1966). Surfaces of unit Qg3 show subdued bar and swale morphology and an intermediate degree of desert pavement development. Similarly, clasts on Qg3 are less cemented than those on Qg2 and the thickness of the Av-horizon is similar or thinner compared to Qg2 (Hunt and Mabey, 1966). Deposits of unit Qg4 are present in modern washes and differ clearly from units Qg2 and Qg3 by the lack of desert pavement and desert varnish (Hunt and Mabey, 1966). Deposits of unit Qg4 show a well-developed bar and swale morphology originating from primary debris-flow depositional forms. Hooke (1972) introduced additional criteria such as the degree of fan dissection and surface relief, which led to a further subdivision of the units. A number of subsequent studies have sought to assign absolute ages to this relative chronology (e.g., Klinger, 2001; Frankel et al., 2007a; Frankel et al., 2007b; Sohn et al., 2007; Machette et al., 2008; Owen et al., 2011; Frankel et al., 2015). Indirect dating of fan surfaces by dating shoreline tufas developed on bedrock along the Black Mountains south of Badwater using U-series techniques (Ku et al., 1998), and correlation with Hunt and Mabey's unit Qg2, led to the suggestion that Qg2 is younger than MIS 6 (Knott et al, 2002). Other correlations of Hunt and Mabey's stratigraphic fan units with numeric dates (e.g., Klinger, 2001; Sohn et al., 2007; Machette et al., 2008; Owen et al., 2011; Sohn et al., 2014 Frankel et al., 2015) suggest that units Qg4 and Qg3 are Holocene in age, and support the hypothesis that Qg2 was deposited in late Pleistocene time.

The first cosmogenic ^{10}Be and ^{26}Al measurements on western Death Valley fans were published by Nishiizumi et al. (1993). They analyzed samples from alluvial fan units Q3a, Q2a, and Q1b on the Hanaupah Canyon fan and from units Q1b and Q2a on the Galena Canyon fan (Fig. 1; Table 1), based on an alluvial fan unit map by Dorn (1988). Minimum ages on the Hanaupah fan

281 are 145.8±10.9 ka (Q3a), 325.5±24.7 ka (Q2a), and 383.4±30.8 ka (Q1b). On the Galena
282 Canyon fan the two measured minimum ages are 403.1±36.8 ka (Q1b) and 410.1±29.2 ka
283 (Q2a). These dates have been recalculated with CRONUS calculator
284 (http://hess.ess.washington.edu/math/; version 2.2; Balco et al., 2008) applying the production
285 rate calibration by Heyman (2014) and the time-variant scaling model by Lal (1991) and Stone
286 (2000). Machette et al. (2008) sampled depth-profiles for cosmogenic ^{36}Cl to measure numeric
287 ages on the Hanaupah Canyon, Trail Canyon, and Galena Canyon fans. They took six samples
288 from one single fan unit (Qai) and one sample from the slightly older fan unit Qlm on the
289 Hanaupah Canyon fan. In addition, they took two samples from unit Qai on the Galena Canyon
290 fan and one sample each from units Qai and Qaio on the Trail Canyon fan (Fig. 1; Table 1). The
291 two profiles on the Galena Canyon fan yielded best-fit profile ages of 47 ka and 84 ka for unit
292 Qai. Five profiles on the Hanaupah Canyon fan gave best-fit ages of 39 ka, 66 ka, 72 ka, 96 ka
293 (all unit Qai), and 130 ka (unit Qlm), and one rock sample had an age of 118±11 ka (Qai). Unit
294 Qaio on the Trail Canyon fan yielded the oldest best-fit depth-profile age at 171 ka and the rock
295 sample from unit Qai had an age of 102±7 ka (Machette et al., 2008). Another set of numeric
296 results comes from Liu and Broecker who applied the varnish microlamination (VLM) dating
297 technique on the Galena Canyon, Hanaupah Canyon, Six Spring Canyon and Warm Springs fans.
298 They measured 13 samples from Bull's (1991) fan units Q2a, Q2b, and Q2c (Table 1) and
299 obtained VML ages of 276 ka and 295 ka for unit Q2a, three VML ages between 74 and 165 ka
300 for unit Q2b, and VML ages between 30 and 60 ka for unit Q2c. Among the latter two samples
301 were obtained from the Warm Springs fan.
302

On the eastern side of Death Valley, cosmogenic radionuclide and OSL dates on several alluvial fan surfaces near Badwater and Mormon Point (Fig. 1) are generally younger compared to measurements on the west side alluvial fans (e.g. Machette et al., 2008; Owen et al., 2011; Sohn et al., 2014; Frankel et al., 2015). Most of the dated alluvial fan surfaces yield exposure ages that are younger than 20 ka, while a few samples have dates between 40 and 80 ka (Sohn et al., 2007; Owen et al., 2011; Frankel et al., 2015). Inheritance on these dated alluvial fan surfaces, as measured in samples from the active channels and from cosmogenic depth-profiles, ranges between 6 and 94 ka (Machette et al., 2008; Owen et al., 2011; Frankel et al., 2015), and is thus fairly high compared to the exposure ages of the surfaces themselves.

Table 1. Correlation of mapped fan surface units in Death Valley

		Hunt and Mabey (1966)	Machette et al. (2008)	Nishiizumi et al. (1993)[1]	Bull (1991)[2]
Holocene	(0-10 ka)	Qg4	Qay		Q4b Q4a
		Qg3	Qayo		Q3 (a-c)
Pleistocene	Late (10-130 ka)	Qg2	Qai	Q3a	Q2c
			Qlm		Q2b
	Middle (130-780 ka)		Qaio Qao	Q2a	Q2a
				Q1b	
	Early (>780 ka)	QTg1	QTa		

[1]The fan surface units are based on Dorn (1988).
[2] Units were originally based on the Lower Colorado River region, but applied to the Death Valley region.

323 ## 4. Methods

324 ### 4.1. Mapping of fan surfaces

325 In order to establish a relative chronology to guide our sample collection, we mapped distinct
326 depositional fan surface units using similar criteria to those applied in previous studies by Denny
327 (1965) and Hunt and Mabey (1966): channel spacing, degree of pavement development, varnish
328 development, and short- and long-wavelength relief on the fan surfaces. Fan areas with similar
329 surface characteristics were mapped as a single surface unit. Surface relief and channel spacing
330 were derived from high-resolution Airborne Laser Swath Mapping (ALSM) data obtained from
331 the National Center for Airborne Laser Mapping. The survey area comprised approximately 25
332 km^2 and contained 25 flight lines each with a scan width of 582.4 m and swath overlap of 260 m.
333 The data were interpolated to a digital elevation model with a spatial resolution of 1 m/pixel and
334 a vertical accuracy of 5-10 cm. Due to the lack of vegetation the data were not filtered for
335 vegetation removal. Short-wavelength relief was defined as elevation variation over a lateral
336 distance of 10 m and reflects roughness on the scale of individual debris-flow channels and
337 deposits. Long-wavelength relief was assessed over a radius of 1000 m and reflects topographic
338 variations due to post-depositional incision of the fan surface units. The degree of pavement and
339 varnish development were qualitatively assessed in the field.

340

341 ### 4.2. Cosmogenic radionuclide exposure dating

342 We dated debris-flow fan surfaces on the Warm Springs fan using the in-situ produced
343 cosmogenic radionuclides ^{10}Be and ^{26}Al. The use of both nuclides allows the identification of
344 complex exposure and burial histories which can potentially complicate the interpretation of ages
345 from depositional surfaces (e.g., Repka et al., 1997; Hancock et al., 1999; Wolkowinsky and

346 Granger, 2004; Matmon et al., 2005; Frankel et al., 2007b; Machette et al., 2008). We collected
347 28 samples from different fan surface units on the Warm Springs fan (Fig. 4; Table 2). Surfaces
348 on the Warm Springs fan have few boulders which could be used as sampling targets (Fig. 3B).
349 Therefore, we amalgamated 30 to 40 individual surface clasts from each sample location (e.g.,
350 Anderson et al., 1996; Repka et al., 1997; Hetzel et al., 2002; Marchetti and Cerling, 2005) in
351 order to statistically average out potential inheritance outliers (Anderson et al., 1996; Repka et
352 al., 1997). We sampled clasts with diameters between 5 and 10 cm. At all sampling sites we
353 collected the same lithology: a fine-grained quartzite. We chose sampling sites on planar fan
354 surfaces with well-developed pavement, well away from hillslopes and channel margins, except
355 in the active channel where we took clasts directly from the wash.
356
357 The exposure of rock in the source area during erosion and transport, prior to final deposition on
358 the fan can result in a significant concentration of inherited cosmogenic nuclides. Thus, the
359 assessment of nuclide inheritance is absolutely essential for the interpretation of surface dates.
360 Measurements of nuclide concentrations from multiple depths at the same site are one way to
361 account for inheritance (Anderson et al., 1996; Repka et al., 1997). When depth sampling is not
362 an option, a less accurate approach is to estimate the nuclide concentration in a sample from the

363 **TABLE 2. ANALYTICAL DATA AND RESULTS FOR ^{10}BE AND ^{26}AL SAMPLES ON THE WARM SPRINGS FAN, DEATH VALLEY**
364

Sample Name ETH	Sample Name	Latitude (°N)	Longitude (°W)	Elevation (m)	Quartz (g) [a]	Be carrier mass (mg)	^{10}Be/^{9}Be x 10^{-12} [b,c,d]	Al carrier mass (mg)	^{26}Al/^{27}Al x 10^{-12} [b,d]
ZB2821	10303-1	35.967	116.854	308	30.3	0.3911	4.70 ± 0.16	3.5100	8.46 ± 0.25
ZB3812	80303_2	35.991	116.813	-13	27.4	0.3973	1.09 ± 0.05	3.1500	2.49 ± 0.11
ZB5430	80303_3	35.9837	116.813	57	26.5	0.4061	2.33 ± 0.05	3.3950	4.76 ± 0.14
ZB3813	80303_4	35.984	116.819	41	27.4	0.3968	1.80 ± 0.06	3.2700	4.17 ± 0.19
ZB2822	90303-2	35.982	116.829	124	29.8	0.3622	3.36 ± 0.12	3.2900	6.88 ± 0.21
ZB2820	190303-1	35.962	116.857	349	30.0	0.4161	4.79 ± 0.14	3.0450	8.79 ± 0.28
ZB3814	110304_6	35.955	116.846	288	27.0	0.3973	3.20 ± 0.10	2.9500	7.88 ± 0.37
ZB3298	120304_1	35.997	116.846	128	29.0	0.3904	2.87 ± 0.09	3.1900	5.37 ± 0.19
ZB3820	120304_2	35.998	116.859	276	25.8	0.3673	3.75 ± 0.14	3.0350	6.88 ± 0.35
ZB3815	120304_4	35.982	116.857	276	27.6	0.3978	3.54 ± 0.16	3.0950	7.55 ± 0.35
ZB3821	130304_1	35.975	116.816	102	31.4	0.3861	3.57 ± 0.11	3.4200	6.89 ± 0.28
ZB3816	130304_3	35.974	116.809	73	26.6	0.3979	2.66 ± 0.08	2.9200	6.47 ± 0.27
ZB3822	150304_1	35.999	116.803	-56	22.6	0.3951	1.15 ± 0.03	3.4750	2.44 ± 0.12
ZB3817	150304_3	35.994	116.808	-21	26.4	0.3969	1.07 ± 0.03	3.1500	2.54 ± 0.11
ZB3299	170304_1	35.998	116.834	73	28.4	0.3988	0.83 ± 0.03	3.2950	2.01 ± 0.09
ZB3818	170304_2	36.014	116.830	-34	27.8	0.3954	1.09 ± 0.03	3.9350	2.05 ± 0.11
ZB3823	180304_1	36.005	116.813	-6	33.5	0.3879	0.93 ± 0.04	4.9050	1.32 ± 0.07
ZB3823	180304_2	36.002	116.812	0	24.2	0.3964	0.71 ± 0.03	2.6350	2.05 ± 0.09
ZB3824	180304_5	35.988	116.842	171	25.4	0.3917	3.51 ± 0.11	2.8700	8.19 ± 0.32
ZB5421	280207_1	35.9611	116.813	415	26.4	0.3993	1.00 ± 0.05	3.7700	2.00 ± 0.09
ZB5422	280207_1A	35.9611	116.813	415	29.2	0.3971	0.43 ± 0.02	3.9400	0.92 ± 0.08
ZB5423	280207_1B	35.9611	116.813	415	27.5	0.3998	0.38 ± 0.02	2.9450	1.17 ± 0.06
ZB5424	280207_2	35.9749	116.813	235	27.1	0.4040	0.61 ± 0.02	3.4450	1.37 ± 0.06
ZB5425	280207_3	35.9687	116.813	310	25.8	0.4048	0.41 ± 0.02	3.9800	0.77 ± 0.04
ZB5426	20307_1	36.002	116.813	-13	28.2	0.4070	0.62 ± 0.02	3.4350	1.39 ± 0.05
ZB5427	20307_1A	36.002	116.813	-13	25.8	0.3983	1.03 ± 0.04	3.1950	2.74 ± 0.10
ZB5428	20307_1B	36.002	116.813	-13	31.6	0.4033	0.59 ± 0.02	3.5900	1.30 ± 0.06
ZB5429	20307_2	36.0055	116.813	-21	32.7	0.4036	0.73 ± 0.02	4.7950	1.10 ± 0.05

365 [a] We used a density of 2.7 g cm^{-3} for all samples.
366 [b] Sample ratios were normalized to S555 (^{10}Be; Kubik and Christl, 2010) and ZAL94 (^{26}Al; Nishiizumi, 2004) standardizations.
367 [c] Blank corrected ^{10}Be/^{9}Be ratio including a correction of 2.54 x 10^{-14} ± 2.12 x 10^{-15} based on the weighed mean of nine process blanks. No correction was applied to the ^{26}Al/^{27}Al
368 ratio.
369 [d] Uncertainty includes 1σ AMS measurement errors, statistical counting error and the uncertainties due to the normalization to the standards and the blank.

active channel, and to use that as a proxy for accumulated inheritance during sample deposition (e.g., Brown et al., 1998; Hetzel et al., 2002; Machette et al., 2008; Owen et al., 2011). This approach assumes constant inheritance accumulation through time, or equivalently a constant mean time required for sample erosion and transport from the sediment source to the fan. Due to National Park restrictions we were unable to excavate alluvial fan surfaces to a sufficient depth for profile sampling. Therefore, we assessed inheritance by collecting 10 amalgamated samples from the active channel at different distances from the catchment outlet. The sampling procedure was the same as for the fan surface samples. To check reproducibility, we took several duplicate samples from the active channel at proximal, mid, and distal fan positions: three at the catchment outlet, two each at 3 and 4.5 km downstream from the outlet, and five at the distal part of the fan, ~7.5 km from the outlet.

All samples were processed at the PSI/ETH Zürich cosmogenic laboratory between 2003 and 2007 using standard techniques according to Kohl and Nishiizumi (1992), Ivy-Ochs (1996), and Ochs and Ivy-Ochs (1997). For our analysis we only took clasts with a thickness of ~2 cm, and we used a rock saw to cut those with larger thicknesses. We crushed and sieved each clast to a grain size of 0.25 to 0.5 mm, from which we took the same mass to contribute to the amalgamated sample. The inherent Al concentration was determined from an aliquot of the solution of the dissolved quartz using ICP-OES measurements carried out at the University of Jena. No additional ^{27}Al was added to our samples. The isotopic ratios were determined by accelerator mass spectrometry (AMS) at PSI/ETH Zürich before April 2010. Concentrations were referenced to ^{10}Be standard 07KNSTD (Kubik and Christl, 2010) and ^{26}Al standard KNSTD (Nishiizumi, 2004). For ^{10}Be we ran nine process blanks and used their weighted mean

393 ratio of 2.54 x 10^{-14} ± 2.12 x 10^{-15} for the blank correction. We did not apply a blank correction to
394 the $^{26}Al/^{27}Al$ ratio. We calculated ^{10}Be and ^{26}Al exposure ages using the CRONUS Earth online
395 exposure age calculator (http://hess.ess.washington.edu/math/, Balco et al., 2008; version 2.2
396 with updated constants based on version 2.2.1) and the time dependent Lal (1991)/Stone (2000)
397 scaling model. We applied the production rate calibration of Heyman (2014) with production
398 rates of 3.94 ± 0.2 atoms g^{-1} SiO_2 yr^{-1} for ^{10}Be and 26.59 ± 1.35 atoms g^{-1} SiO_2 yr^{-1} for ^{26}Al, and
399 assumed a production ratio $^{26}Al/^{10}Be$ of 6.75 (Lal, 1991; Stone, 2000; Heyman, 2014). A ^{10}Be
400 half-life of 1.39 x 10^6 yr (Chmeleff et al., 2010; Korschinek et al., 2010) and a ^{26}Al half-life of
401 7.08 x 10^5 yr (Nishiizumi, 2004) were used for the age calculation. The effect of topographic
402 shielding is less than 0.5%, and therefore we did not include a correction. Given the present and
403 past climatic setting of Death Valley, we did not correct for either snow cover or vegetation
404 cover.
405
406 **5. Results**
407 **5.1. Relative chronology of fan surface units**
408 Following Hunt and Mabey (1966), we divide the Warm Springs fan into three different fan
409 surface units, named Qg2, Qg3, and Qg4 in order of decreasing age. Qg4 is the most recently
410 active unit and shows well-developed bar-and-swale morphology with clear channels and
411 depositional levees. Qg2 and Qg3, in contrast, have surfaces that are modified by post-
412 depositional processes, and do not reflect the original depositional morphology.
413 Fan surface unit Qg2 is located at the proximal part of the fan (Figs. 2 and 4), and comprises the
414 largest fraction of the entire fan area. This unit is incised by channels, which have an average
415 spacing of about 200 m (Figs. 2 and 5) and relief between the channel floors and the interfluves

of up to 50 m (Figs. 2, 5). The surfaces of Qg2 are smooth, and lack obvious bar-and-swale morphology or any debris-flow depositional characteristics, such as channel-levee complexes. Away from the incised channels, the surfaces are planar and have very low short-wavelength relief of several centimeters to a few decimeters.

Well-developed pavements with darkly varnished clasts are partly inset into the underlying fine-grained Av- horizon. Surface unit Qg2 is cut by several faults of the West Side Fault zone, which appear to dip generally eastwards into the basin and show normal displacement. Offsets of the alluvial fan surface are between ~10 and ~60 m across individual fault strands, with the largest offset on a fault located approximately 4 km from the fan head (Fig. 2). To the east of this fault, surface unit Qg2 is substantially less incised, with a long-wavelength relief of less than 20 m (Fig. 2). Near the distal limit of unit Qg2, the paleoshoreline is cut into the surface at an elevation of ~65 m a.s.l. and thus lies topographically higher than unit Qg3 (Fig. 2) (Hooke, 1972; Blair, 1999a; Machette et al., 2008).

Alluvial fan surface unit Qg3 is relatively small in area and forms several individual surface fragments at the distal part of the fan that have been isolated from each other by later incision. These fragments stand a few meters above the presently-active channels. The long-wavelength relief on surface unit Qg3 is significantly smaller than that of surface unit Qg2 and ranges between 2 and 5 m (Fig. 5). In contrast, the short-wavelength surface relief is higher compared with Qg2, on the order of a few decimeters. The surface of unit Qg3 has pavements with darkly-varnished clasts. As fan unit Qg3 is inset below the Warm Springs fan paleoshoreline, Qg3 must be younger, and is therefore probably younger than MIS 6.

439 Fan surface unit Qg4 represents the active depositional surface at the distal part of the Warm
440 Springs fan, including the incised trunk channel that funnels sediment from the catchment outlet
441 downstream into the basin. The long-wavelength relief on this modern surface is less than 2 m
442 (Fig. 5); short-wavelength surface relief is on the order of several decimeters. There is no
443 pavement and no Av horizon developed on this lobe and most clasts lack any apparent coating of
444 desert varnish.
445
446 **5.2. Measurements of ^{10}Be and ^{26}Al from amalgamated clast samples**
447 If we assume no erosion, the ^{10}Be exposure data from the Warm Springs fan surfaces yield
448 apparent exposure dates between 989 ± 43 ka and 125 ± 5 ka, whereas the results from ^{26}Al range
449 from 957 ± 74 ka to 124 ± 6 ka (Figs. 4 and 6; Table 3; all ages reported to ±1σ uncertainty).
450 Dates obtained from both nuclides compare relatively well, especially for samples younger than
451 500 ka. Eleven ^{10}Be dates from the oldest fan unit Qg2 range between 989 ± 43 ka and 628 ± 17
452 ka and are also the oldest measurements on the Warm Springs fan (Fig. 6). Two other dates from
453 Qg2 (272 ± 13 ka and 448 ± 18 ka), however, are younger than all other measurements on this
454 unit. The younger sample was collected from an elevation of -13 m, well below the maximum
455 lake level highstand during MIS 6 (Hooke, 1972; Blair, 1999a; Forester et al., 2005), and
456 therefore could have been affected by reworking through wave action during the lake phase. The
457 older sample originates from the hanging wall of a west-dipping normal fault with a vertical
458 surface offset of about 15 m. It is possible that this sample has been affected by reworking
459 associated with fault motion and fault scarp degradation. ^{10}Be exposure dates on unit Qg3 range
460 from 369 ± 13 ka to 180 ± 8 ka and four out of five samples have dates between 280 ± 10 ka and
461 180 ± 8 ka (Figs. 4 and 6).

462 The ten samples from the presently active, incised channel of unit Qg4 yield ^{10}Be concentrations
463 ranging from 3.69 ± 0.2 x 10^5 to 10.7 ± 0.4 x 10^5 ^{10}Be atoms g^{-1} and ^{26}Al concentrations that range
464 between 26.5 ± 1.4 x 10^5 and 75.7 ± 2.9 x 10^5 atoms g^{-1} (Table 3). Figure 7 shows the pattern of
465 measured ^{10}Be concentrations along the active channel. While the spread of concentrations at the
466 catchment outlet and at the distal part of Qg4, where we took multiple samples, varies by a factor
467 of 2 to 3, measured concentrations tend to be lower at the fan head compared to those at the fan
468 toe. When we scale ^{10}Be concentrations to the local production rate at the sampling site, the
469 calculated ^{10}Be exposure dates would range between 63 ± 3 ka and 174 ± 9 ka at the catchment
470 outlet and between 125 ± 5 ka and 275 ± 12 ka at the fan toe. The equivalent ^{26}Al dates range
471 between 70 ± 7 ka and 168 ± 9 ka at the fan head and between 124 ± 6 ka and 310 ± 15 ka at the
472 distal position of the fan.
473
474 Two-nuclide erosion island plots elucidate the erosional history of the dated landform (or
475 boulder) and complex histories through burial and exposure (Fig. 8). The upper curve of a two-
476 nuclide erosion island plot delineates the trajectory of a sample with increasing age but
477 undergoing no erosion. As soon as the sample is affected by erosion the trajectories move below
478 the zero-erosion line and show lower ^{26}Al/^{10}Be ratios, respectively. These trajectories will
479 continue until an isotopic equilibrium is reached, where production and decay of cosmogenic
480 nuclides are balanced. Samples reveal a simple exposure history, when they fall between the
481 non-erosion and equilibrium curve, or they plot exactly on both curves. The history of a sample
482 is more difficult to reconstruct if the sample falls below the 'erosion-island' in the 'complex
483 field'. Samples within the complex field have experienced at least one period of burial, coverage,
484 or significant (on the order of several 10 cm) erosion by spalling. The plot of ^{26}Al/^{10}Be ratio

485 against ^{10}Be shows that 22 out of 26 samples fall within ±1σ of the model curve for constant
486 exposure (Fig. 8). Four samples (20307_2, 120304_1, 120304_2, and 190303_1), with calculated
487 dates of 152.2 ± 5.9 ka, 640.2 ± 24.6 ka, 811.4 ± 41.9 ka, and 989.1 ± 42.9 ka, fall below the
488 equilibrium curve (Fig. 8, Table 3). Two samples (280207_1B and 20307_1A), with apparent
489 exposure dates of 62.7 ± 2.9 ka and 274.8 ± 12.2 ka, plot above the constant exposure curve in the
490 'forbidden field', which may be related to the chemical processing of the samples. When
491 including the model curve for erosion, all samples except 280207_1B, 20307_1A, 120304_1, and
492 190303_1 fall within ±1σ of the 'erosion island' (Fig. 8, Table 3), and all samples fall within the
493 erosion island when we also consider the errors on both production rates (Stone, 2000). We infer
494 from these results that the majority of our samples record a single-stage, continuous exposure
495 history (Fig. 8). Samples 190303_1 and 120304_1 indicate a limited period of burial, because
496 both clearly plot below the 'erosion island'.
497
498
499
500
501
502

503

504 **TABLE 3. ^{10}BE AND ^{26}AL MEASUREMENTS ON THE WARM SPRINGS FAN, DEATH VALLEY**
505

Sample Name	Fan unit	^{10}Be (10^5 atoms g^{-1} qtz)[a]	^{10}Be date (ka) [a,b]	^{26}Al (10^5 atoms g^{-1} qtz)[a]	^{26}Al date (ka) [a,b]	^{26}Al/^{10}Be
10303_1	Qg2	40.68 ± 1.4	923.9 ± 45.6 (72.5)	219.05±6.7	871.0 ± 49.2 (81.8)	5.39 ± 0.25
80303_2	Qg2	10.58 ± 0.5	272.5 ± 13.3 (19.4)	63.9±2.9	255.2 ± 14.0 (19.7)	6.04 ± 0.38
80303_3	Qg2	23.82 ± 0.5	628.4 ± 16.8 (40.6)	135.81±4.3	595.4 ± 2.2 (48.4)	5.71 ± 0.22
80303_4	Qg2	17.40 ± 0.6	447.8 ± 17.8 (30.5)	110.96±0.5	468.1 ± 29.1 (40.5)	6.38 ± 0.36
90303_2	Qg2	27.33 ± 1.0	689.7 ± 31.3 (50.9)	169.67±5.2	753.6 ± 38.1 (66.1)	6.21 ± 0.29
190303_1	Qg2	44.42 ± 1.3	989.1 ± 42.9 (75.5)	198.75±6.5	712.8 ± 38.3 (62.2)	4.48 ± 0.20
110304_6	Qg2	31.47 ± 1.0	687.7 ± 27.1 (48.5)	192.33±9.2	733.5 ± 58.2 (74.8)	6.12 ± 0.35
120304_1	Qg2	25.79 ± 0.8	640.2 ± 24.6 (44.6)	131.69±4.8	527.2 ± 27.5 (43.2)	5.11 ± 0.24
120304_2	Qg2	35.68 ± 1.4	811.4 ± 41.9 (63.6)	180.19±9.3	677.2 ± 56.0 (69.7)	5.06 ± 0.32
120304_4	Qg2	34.11 ± 1.5	770.5 ± 46.3 (64.0)	188.77±9.1	724.1 ±57.5 (73.8)	5.54 ± 0.37
130304_1	Qg2	29.33 ± 0.9	772.0 ± 30.6 (55.7)	167.41±7.0	761.1 ± 52.4 (74.3)	5.71 ± 0.29
130304_3	Qg2	26.63 ± 0.8	706.0 ± 27.6 (50.1)	158.70±6.8	729.1 ± 50.6 (70.7)	5.97 ± 0.31
150304_1	Qg3	13.38 ± 0.4	368.8± 13.1 (24.0)	83.75±4.1	368.4 ± 23.0 (31.1)	6.27 ± 0.36
150304_3	Qg3	10.78 ± 0.3	280.4 ± 9.8 (17.9)	67.56±2.9	274.3 ± 14.6 (21.0)	6.27 ± 0.33
170304_1	Qg3	7.80 ± 0.3	181.6 ± 8.6 (12.6)	51.98±2.5	185.5 ± 10.3 (14.1)	6.67 ± 0.42
170304_2	Qg3	10.37 ± 0.3	272.5 ± 9.5 (17.3)	64.71±3.7	265.1 ± 18.3 (23.1)	6.25 ± 0.40
180304_1	Qg3	7.20 ± 0.3	180.4 ± 8.2 (12.3)	43.14±2.2	164.0 ± 9.7 (12.9)	6.00 ± 0.40
180304_2	Qg4	7.71 ± 0.3	192.2 ± 8.7 (13.1)	49.65±2.1	189.8 ± 9.4 (13.8)	6.44 ± 0.38
180305_5	Qg2	36.15 ± 1.1	924.5 ± 38.8 (69.4)	206.39±8.3	957.3 ± 74.0 (102.9)	5.72 ± 0.29
280207_1	Qg4	10.07 ± 0.5	173.8 ± 9.1 (12.5)	63.67±2.9	167.8 ± 8.9 (12.3)	6.33 ± 0.41
280207_1A	Qg4	3.85 ± 0.2	65.4 ± 3.4 (4.7)	27.59±2.3	70.1 ± 6.5 (7.1)	7.18 ± 0.70
280207_1B	Qg4	3.69 ± 0.2	62.7 ± 2.9 (4.2)	27.97±1.4	71.1 ± 4.0 (5.3)	7.60 ± 0.50
280207_2	Qg4	6.07 ± 0.2	120.1 ± 4.7 (7.7)	38.78±1.7	115.9 ± 5.7 (8.2)	6.39 ± 0.36
280207_3	Qg4	4.24 ± 0.2	78.8 ± 4.4 (5.8)	26.52±1.4	73.7 ± 4.3 (5.6)	6.27 ± 0.46
20307_1	Qg4	5.97 ± 0.2	149.2 ± 5.8 (9.6)	37.76±1.3	142.7 ± 5.8 (9.5)	6.33 ± 0.32
20307_1A	Qg4	10.66 ± 0.4	274.8 ± 12.2 (18.9)	75.68±2.9	310.0 ± 15.2 (23.2)	7.11 ± 0.39
20307_1B	Qg4	5.02 ± 0.2	124.5 ± 4.9 (8.0)	33.10±1.4	124.0 ± 6.1 (8.8)	6.60 ± 0.37
20307_2	Qg4	6.04 ± 0.2	152.2 ± 5.9 (9.8)	36.00±1.5	136.6 ± 6.4 (9.6)	5.97 ± 0.33

506 [a] Uncertainty includes 1σ AMS measurement errors, statistical counting error, uncertainty due to the normalization of the standards and the blank, and for ^{26}Al the ICP-OES
507 measurement uncertainty.
508 [b] Exposure ages were calculated with the CRONUS-Earth exposure age calculator (http://hess.ess.washington.edu/math/, Balco et al., 2008 and update from v. 2.1. to v. 2.2) and
509 time-dependent Lal (1991)/Stone (2000) scaling model using the production rate calibration set by Heyman (2014). A ^{10}Be half-life of 1.39 x 10^6 years (Korschinek et al., 2010;
510 Chmeleff et al., 2010) and a ^{26}Al half-life of 7.08 x 10^5 years (Nishiizumi, 2004) were used for the age calculation. Uncertainties in parentheses include propagated production rate
511 scaling uncertainty.

6. Discussion

6.1. Surface unit chronology on the Warm Springs fan

The results from measured ^{10}Be and ^{26}Al concentrations show that surfaces of the Warm Springs fan record a depositional history that extends back into the early Pleistocene. Based on the observation that most samples fall within ±1σ of the 'erosion island' (Fig. 8, Table 3), we infer that the fan surfaces mostly underwent a simple exposure history. This implies that the early and middle Pleistocene surfaces have been relatively stable since they were abandoned and that they have been affected only by slow erosion. If we assume that our oldest sample (190303_1) with the highest measured ^{10}Be concentrations is in secular equilibrium, the maximum erosion rate that we could infer from the ^{26}Al/^{10}Be ratio is 0.6 ± 0.03 m Ma^{-1}. We have, however, no constraints to determine whether our samples are in secular equilibrium or not. Therefore, we interpret our apparent exposure dates conservatively as minimum ages as even small amounts of erosion will shift the results towards older ages.

Our interpretation of apparent surface exposure dates as minimum ages for surface abandonment must also account for the possible influence of inheritance (e.g., Anderson et al., 1996; Repka et al., 1997; Hancock et al., 1999; Wolkowinsky and Granger, 2004; Matmon et al., 2005). The results from the active channel samples show that fan surface samples on the Warm Springs fan contain a significant inherited radionuclide component, as previously documented for other localities in Death Valley (Machette et al., 2008; Owen et al., 2011; Frankel et al., 2015). Inheritance in the Warm Springs fan could be derived from three different potential sources. First, depending on the residence time of sediment in the headwaters, the fan catchment could contribute a significant amount of inheritance. The upper Warm Springs catchment contains a low-relief area that has likely acted as temporary sediment storage (Fig. 1). Second, inheritance could be derived from exposure during transport in the active channel. Third, incision and erosion of older fan surface units could

538 contribute high-inheritance clasts to sediments in the active channel. This last mechanism
539 might be particularly important where the channel cuts through old fan surface deposits with
540 high radionuclide concentrations at the surface.
541
542 Measurements of ^{10}Be in the active channel show that, while radionuclide concentrations
543 in replicate samples vary by a factor of 2 to 3, the concentrations generally increase with
544 increasing distance from the catchment outlet (Fig. 7). Substantial concentrations of
545 cosmogenic ^{10}Be and ^{26}Al measured at the catchment outlet suggest that pre-exposure of the
546 sediment in the catchment is a likely source for inheritance. The downstream increase in
547 concentration along the active channel could be due either to exposure during transport, or to
548 progressive incorporation of old, high-concentration sediment derived from erosion of the fan
549 surface units. Comparison of cosmogenic concentrations in samples from the fan surfaces
550 with samples from the active channel at 3 and 4.5 km distance from the catchment outlet,
551 however, show that channel samples contain only 10-20% of the concentrations measured in
552 the fan surface samples. While the incision of the debris-flow fan indicates that channel wall
553 clasts must have contributed to the channel sediments, the nuclide signal suggests that the
554 contribution of old clasts from the fan surfaces into modern alluvium does not significantly
555 increase the amount of inheritance. One reason could simply be that most channel wall clasts
556 are shielded below the depth of the cosmogenic production zone, and therefore these clasts do
557 not carry a substantial cosmogenic signal when they enter the channel floor. Another reason
558 could be that clasts derived from the channel incision have already largely been removed from
559 the active channel and have been incorporated into the deposits of unit Qg3. This would
560 imply that most clasts in the modern channel are derived directly from the catchment area.
561 Based on our data, we cannot explicitly determine the source of inheritance, but most likely
562 all three components (pre-exposure in the catchment, exposure during transport, and input
563 from the channel walls) contribute to the total inherited signal.

We can use the measured inherited concentrations from the channel samples to define boundaries for the timing of fan surface activity. Correcting the dates on fan unit Qg2 with the minimum inheritance value of 63±3 ka (280207_1B) measured at the catchment outlet would lower the measured exposure dates by less than 10% for samples that are 600 ka or older. For the maximum inheritance correction of 174±9 ka (280207_1) also measured at the catchment outlet, the calculated dates would decrease by 20 to 30%. Thus, the measured exposure dates are likely to be close to the true depositional ages on Qg2, as long as the amount of inheritance measured at the catchment outlet has not varied significantly through time.

On unit Qg3, we can approximate depositional ages based on the mean inheritance of our five distal samples 180304_2, 20307_1, 20307_1A, 20307_1B, and 20307_2. This yields a correction of 178 ± 59 ka, which shifts measured fan surface dates from unit Qg3 to significantly younger dates. In comparison, the mean surface date of unit Qg3 yields 256±78 ka. After the subtraction of mean inheritance from each individual Qg3 sample, four samples postdate MIS 6 (101 ka, 93 ka, 3 ka, and 1 ka) and one sample has an age of 190 ka. Two samples dated on unit Qg3 using varnish microlaminations as dating technique yield 60 ka (Liu and Broecker, 2008). These results fit the expectation that unit Qg3 postdates the MIS 6 paleoshoreline on the Warm Springs fan. The uncertainty in the appropriate inheritance correction, and the large inherited concentrations relative to measured sample concentrations, mean that the exact timing of fan activity cannot be determined, and therefore at present we can only limit the period of fan activity during Qg3 deposition to the late Pleistocene and Holocene. For unit Qg4, these results imply that fan activity occurred throughout the Holocene.

6.2 Comparison with previous surface chronologies on the Warm Springs fan

Our surface mapping largely agrees with the relative chronology published by Hunt and

590 Mabey (1966). With a few differences on the distal fan, we placed the boundary of unit Qg2
591 on the proximal and central part of the Warm Springs fan very near the boundary defined by
592 Hunt and Mabey (1966). Our unit Qg3, however, covers significantly less surface area
593 compared to their interpretation. The major difference is the large area at the fan toe, which
594 we map as unit Qg4 while Hunt and Mabey (1966) identified several individual Qg3 "islands"
595 separated by unit Qg4. This difference in the separation of individual fan units results from
596 our analysis of surface roughness using the Lidar dataset, which shows lower long-
597 wavelength relief on Qg4 compared to Qg3.
598
599 The suggested age boundaries for Hunt and Mabey's stratigraphic units Qg2, Qg3 and Qg4
600 range from the late Pleistocene (10-130 ka; Qg2) to the early Holocene (Qg3) and the late
601 Holocene (Qg4) (Klinger, 2001; Machette and Crone, 2001; Knott et al., 2002; Machette et
602 al., 2008; Owen et al., 2011; Frankel et al., 2015). Given that on Warm Springs fan units Qg3
603 and Qg4 the uncertainties due to inheritance and measurement errors are too high to allow a
604 reliable correction and comparison with the proposed stratigraphic ages, we can only use our
605 measured surface dates on unit Qg2 to roughly correlate these dates with the stratigraphic
606 ages. For unit Qg2, the majority of dates, when we include a correction for inheritance based
607 on the measurements in the active channel, overlaps with early to middle Pleistocene time.
608 This implies that surfaces that we mapped as unit Qg2 are much older compared to the
609 proposed stratigraphic late Pleistocene age of Qg2 (Knott et al., 2002). In fact, the dates on
610 unit Qg2 agree with the suggested timing of the older stratigraphic unit Q1 (Knott et al.,
611 2005). Certainly, given that unit Qg2 must be younger than MIS 6 (Knott et al., 2002), the
612 time constraints measured on our mapped unit Qg2 would fit the stratigraphic time boundaries
613 for unit Q1 much better (Knott et al., 2005; Machete et al., 2008). However, the morphologic
614 description of surface unit Q1 does not entirely fit our field observations. While the lack of
615 bar-and-swale morphology and the high degree of surface dissection on our mapped unit Qg2

616 is also characteristic for the morphologic description of unit Q1, rock varnish and desert
617 pavement are well-developed on the oldest Warm Springs fan surfaces but are described to be
618 only weakly preserved on the Q1 surfaces (Hunt and Mabey, 1966; Knott et al., 2005). When
619 we ignore the morphologic descriptions of the fan units, the existing time constraints on unit
620 Qg2 elsewhere in the region (Knott et al., 2002) and the numeric data we obtained from our
621 mapped Qg2 unit appear to suggest that Warm Springs fan unit Qg2 would correctly be
622 labeled as the stratigraphically older unit Q1. This is turn would imply that all stratigraphic
623 units on the Warm Springs fan would have to be revised.
624
625 **6.3 Evolution of fan morphology and depositional pattern on the Warm Springs fan**
626 Overall, the numeric dates on our oldest mapped fan surface unit Qg2 are consistent with
627 deposition over a long period of more than $4x10^5$ years until fan activity shifted basinward to
628 form a new debris-flow fan unit. Assuming that our measured cosmogenic dates are a
629 reasonable proxy for an approximate time window of fan surface activity, the spatial
630 distribution of these dates across Qg2 shows that fan activity probably shifted laterally over
631 time as one would expect for a debris-flow dominated fan (e.g. Suwa and Okua, 1983;
632 Dühnforth et al., 2007, Ventra and Nichols, 2014; D'Arcy et al., 2015; Schürch et al., 2016).
633 The uncertainty on the cosmogenic measurements and the unknown inheritance at each
634 sampling location, however, do not allow us to interpret our results as true depositional ages.
635 In addition, the lack of distinct morphologic differences on the oldest surface prevents any
636 more detailed identification of individual debris-flow lobes or units as typically found on
637 younger debris-flow fans, where lateral shifts in deposition and cross-cutting relationships
638 allow temporal reconstruction of debris-flow activity (e.g. Dühnforth et al., 2007; Schürch et
639 al., 2016). Clearly, evidence for radial shifts in the locus of fan deposition (from unit Qg2 to
640 Qg3 to Qg4), as also seen at Illgraben (Schürch et al., 2016) and in debris-flow fan
641 experiments by de Haas et al. (2016), are preserved on the Warm Springs fan. The radial shift

642 in deposition results from the incision of the Warm Springs fan head. The incision represents
643 a major change in the geologic history of the fan as the sedimentary system shifted from
644 aggradation to entrenchment and the depocenter shifted out into the basin leading to the
645 preservation of the older depositional surfaces (e.g. Hooke, 1967; Blair, 1999a, 1999b;
646 Harvey, 2005; Dühnforth et al., 2007). The driver for fan head incision in this setting has been
647 the subject of much debate, and unfortunately our age constraints are not sufficiently precise
648 to discriminate between different potential models. According to Denny (1965) and Hooke
649 (1972), the eastward tilting of the valley floor in the hanging wall of the BMFZ led to base
650 level lowering with the subsequent entrenchment of the fan heads on the western side of
651 Death Valley. It may also be possible that drawdown of the MIS 6 lake level highstand drove
652 incision of the Warm Springs fan and of other debris-flow fans along the west side of Death
653 Valley, as has been proposed for other alluvial fans along the shoreline of Lakes Lahontan
654 and Mojave in the western United States (Harvey et al., 1999; Ritter et al., 2000; Harvey,
655 2005). Following incision of the Warm Springs fan head, the depocenter during late
656 Pleistocene und Holocene time has been located near the fan toe leading to surface unit
657 deposition and reworking. It is clear that the reoccupation of the oldest proximal and central
658 surfaces on the Warm Springs fan, and resurfacing across the proximal fan, will only occur if
659 there is substantial aggradation in the incised channel and backstepping of the depocenter
660 (e.g., de Haas et al., 2016; Schürch et al., 2016).
661
662 Based on field observations and analysis of the Lidar dataset, we find that the long-
663 wavelength relief of the fan surfaces increases from the youngest to the oldest unit while the
664 short-wavelength relief decreases. For example, while the youngest unit Qg4 shows clear bar-
665 and-swale morphology, the next oldest unit Qg3 lacks well-preserved channel-levee
666 morphology, and surfaces instead are relatively planar with incipient development of desert
667 pavement and rock varnish. We interpret these observations as an evidence for progressive

surface smoothing by aeolian inflation and diffusive processes and surface dissection, which have likely varied in effect and intensity through time (Wells et al., 1987; Bull, 1991; Ritter et al., 1993; Matmon et al., 2006; Frankel and Dolan, 2007; Regmi et al., 2014).

Existing numerical constraints on the time scale of surface smoothing of primary debris-flow morphology on an alluvial fan suggest that it takes more than 280 ka on alluvial fans in the Mojave Desert (Matmon et al., 2006) and about 70 ka on fans in northern Death Valley (Frankel and Dolan, 2007). When we compare surface relief on the Warm Springs fan units Qg4 to Qg2, we find that debris-flow morphology is completely eliminated within a few 10^5 years. Due to inheritance we are not able to resolve a more precise time scale it takes for smoothing. Even though our results are comparable to Matmon et al. (2006), we argue that local difference in the climatic situation or other local factors, for example differences in the grain size distribution, could be responsible for the difference in the timescale of smoothing.

7. Conclusions

Dating of debris-flow surfaces on the Warm Springs fan in Death Valley, California, using cosmogenic ^{10}Be and ^{26}Al shows that this fan preserves one of the longest chronologies in the southwestern United States. The samples yield early to late Pleistocene dates ranging between 990-630 ka for the oldest mapped fan surface unit (Qg2) and 370-180 ka for the younger fan surface unit Qg3, excluding a correction for inheritance. The amount of inheritance, measured in the active channel, increases from ~65 ka at the catchment outlet to up to 275 ka at the distal fan, which implies that our measured ^{10}Be and ^{26}Al dates cannot be interpreted as true depositional ages.

While the youngest, presently active fan surface unit Qg4 shows clear bar-and-swale morphology, the older surfaces Qg2 and Qg3 have undergone post-depositional, short-wavelength smoothing of original, primary debris-flow depositional forms. At the same time, older fan surfaces are progressively more dissected by a tributary channel network that leaves

694 the oldest surfaces increasingly isolated and protected from younger deposition and
695 resurfacing. We propose that debris-flow fan surfaces on the west side of Death Valley are
696 undergoing continuous surface smoothing, albeit at ever-decreasing rates as the surface
697 becomes smoother through time, while dissection of fan surfaces occurs. As such the Warm
698 Springs fan represents a good example for existing models of surface modification, in which
699 surfaces initially become smoother through time while dissection of the surfaces becomes
700 deeper with increasing age. This system of surface modification through time can only be
701 reset by aggradation in the active channel and backstepping of the active depocenter onto the
702 formerly abandoned part of the fan, such that renewed debris-flow deposition can occur. Our
703 results highlight the complications and limitations inherent in extracting information on long-
704 term fan evolution and palaeo-flow behavior from old debris-flow fans, especially in cases
705 where the primary depositional morphology is eliminated and estimation of the timing of fan
706 deposition is complicated by high uncertainties and high inheritance.
707

708 **8. Acknowledgement**

709 This project was funded by the Swiss National Science Foundation (grants 2100-067624 and
710 200020-105225/1). We would like to thank B. Bookhagen, and C. Matter for field assistance.
711 We greatly appreciate the support of Death Valley National Park service for permitting our
712 research activities on the Warm Springs fan. We also thank Jeffrey Knott, Martin Stokes, two
713 anonymous reviewers, and the editor Scott Lecce for constructive reviews that helped to
714 improve and focus the manuscript.
715
716
717
718
719

720 **9. References**

721 Anderson, R.S., Repka, J.L., Dick, G.S., 1996. Explicit treatment of inheritance in dating
722 depositional surfaces using in situ ^{10}Be and ^{26}Al. Geology 24, 47–51. doi:10.1130/0091-
723 7613(1996)024<0047:ETOIID>2.3.CO.

724 Balco, G., Stone, J.O., Lifton, N.A., Dunai, T.J., 2008. A complete and easily accessible
725 means of calculating surface exposure ages or erosion rates from ^{10}Be and ^{26}Al
726 measurements. Quaternary Geochronology 3, 174–195.
727 doi:10.1016/j.quageo.2007.12.001.

728 Bierman, P.R., Gillespie, A.R., Caffee, M.W., 1995. Cosmogenic ages for earthquake
729 recurrence intervals and debris flow fan deposition, Owens Valley, California. Science
730 270, 447-450. doi: 10.1126/science.270.5235.447.

731 Blair, T.C., 1999a. Sedimentology of the debris-flow-dominated Warm Spring Canyon
732 alluvial fan, Death Valley, California. Sedimentology 46, 941–965. doi:10.1046/j.1365-
733 3091.1999.00260.x.

734 Blair, T.C., 1999b. Cause of dominance by sheetflood vs. debris-flow processes on two
735 adjoining alluvial fans, Death Valley, California. Sedimentology 46, 1015–1028.
736 doi:10.1046/j.1365-3091.1999.00261.x.

737 Blair T.C., McPherson J.G., 1994. Alluvial fan processes and forms. In: Abrahams, A.D.,
738 Parsons A.J. (Ed.), Geomorphology of Desert Environments. Chapman & Hall, London,
739 pp 354–402.

740 Brown, E.T., Bourlès, D.L., Burchfiel, B.C., Raisbeck, G.M., 1998. Estimation of slip rates in
741 the southern Tien Shan using cosmic ray exposure dates of abandoned alluvial fans.
742 Geological Society of America Bulletin 110, 377–386. doi: 10.1130/0016-
743 7606(1998)110<0377:EOSRIT>2.3.CO;2.

744 Bull, W.B., 1964. Geomorphology of segmented alluvial fans in western Fresno County,
745 California. Geological Survey Professional Paper 352, 129 pp.

746 Bull, W.B., 1977. The alluvial fan environment. Progress in Physical Geography 1, 222-270.
747 doi: 10.1177/030913337700100202.
748 Bull, W.B., 1991. Geomorphic responses to climatic change. Oxford University Press, New
749 York, 326pp.
750 Chmeleff, J., von Blanckenburg, F., Kossert, K., Jakob, D., 2010. Determination of the 10Be
751 half-life by multicollector ICP-MS and liquid scintillation counting. Nuclear Instruments
752 and Methods in Physics Research B 268, 192-199.
753 Clarke, L.E., Quine, T.A., Nicholas, A., 2010. An experimental investigation of autogenic
754 behaviour during alluvial fan evolution. Geomorphology 115, 278-285. doi:
755 10.1016/j.geomorph.2009.06.033.
756 de Haas, T., van den Berg, W., Braat, I., Kleinhans, M.G., 2016. Autogenic avulsion,
757 channelisation, and backfilling dynamics of debris-flow fans. Sedimentology 63, 1596-
758 1619. doi: 10.1111/sed.12275.
759 Denny, C.S., 1965. Alluvial fans in the Death Valley region, California and Nevada. U.S.
760 Geological Survey Professional Paper 466, 62 pp.
761 D'Arcy, M., Roda Boluda, D.C., Whittaker, A.C., Carpineti, A., 2015. Dating alluvial fan
762 surfaces in Owens Valley, California, using weathering fractures in boulders. Earth
763 Surface Processes and Landforms 40, 487-501. doi: 10.1002/esp.3649.
764 Dorn, R.I., 1988. A rock varnish interpretation of alluvial-fan development in Death Valley,
765 California. National Geographic Research 4, 56-73.
766 Dühnforth, M., Densmore, A.L., Ivy-Ochs, S., Allen, P.A., Kubik, P.W., 2007. Timing and
767 patterns of debris-flow deposition on Shepherd and Symmes Creek fans, Owens Valley,
768 California, deduced from cosmogenic 10Be. Journal of Geophysical Research – Earth
769 Surface 112. doi:10.1029/2006JF000562.
770 Dühnforth, M., Densmore, A.L., Ivy-Ochs, S., Allen, P.A., 2008. Controls on sediment
771 evacuation from glacially modified and unmodified catchments in the eastern Sierra

772 Nevada, California. Earth Surface Processes and Landforms 33, 1602–1613.
773 doi:10.1002/esp.1694.
774 Forester, R.M., Lowenstein, T.K., Spencer, R.J., 2005. An ostracode based paleolimnologic
775 and paleohydrologic history of Death Valley: 200 to 0 ka. Geological Society of
776 America Bulletin 117, 1379–1386. doi: 10.1130/B25637.1.
777 Frankel, K.L., Dolan, J.F., 2007. Characterizing arid-region alluvial fan surface roughness
778 with airborne laser swath mapping digital topographic data. Journal of Geophysical
779 Research - Earth Surface 112. doi:10.1029/2006JF000644.
780 Frankel, K.L., Dolan, J.F., Finkel, R.C., Owen, L.A., Hoeft, J.S., 2007a. Spatial variations in
781 slip rate along the Death Valley-Fish Lake Valley fault system determined from LiDAR
782 topographic data and cosmogenic ^{10}Be geochronology. Geophysical Research Letters 34,
783 L18303. doi:10.1029/2007GL030549.
784 Frankel, K.L., Brantley, K.S, Dolan, J.F., Finkel, R.C., Klinger, R., Knott, J., Machette, M.,
785 Owen, L.A., Phillips, F.M., Slate, J.L, Wernicke, B.P., 2007b. Cosmogenic ^{10}Be and ^{36}Cl
786 geochronology of offset alluvial fans along the northern Death Valley fault zone:
787 Implications for transient strain in the eastern California shear zone. Journal of
788 Geophysical Research - Solid Earth 112. doi:10.1029/2006JB004350.
789 Frankel, K.L., Owen, L.A., Dolan, J.F., Knott, J.R., Lifton, Z.M., Finkel, R.C., Wasklewicz,
790 T., 2015. Timing and rates of Holocene normal faulting along the Black Mountains fault
791 zone, Death Valley, USA. Lithosphere 8, 3-22. doi: 10.1130/L464.1.
792 Gordon, I., Heller, P.L., 1993. Evaluating major controls on basinal stratigraphy, Pine Valley,
793 Nevada. Geological Society of America Bulletin 105, 47–55. doi: 10.1130/0016-
794 7606(1993)105<0047:EMCOBS>2.3.CO;2.
795 Gray, H.J., Owen, L.A., Dietsch, C., Beck, R.A., Caffee, M.A., Finkel, R.C., Mahan, S.A.,
796 2014. Quaternary landscape development, alluvial fan chronology and erosion of the

797 Mecca Hills at the southern end of the San Andreas fault zone. Quaternary Science
798 Reviews 105, 66-85. doi: 10.1016/j.quascirev.2014.09.009.
799 Hancock, G.S., Anderson, R.S., Chadwick, O.A., Finkel, R.C., 1999. Dating fluvial terraces
800 with 10Be and 26Al profiles: Application to the Wind River, Wyoming. Geomorphology
801 27, 41–60. doi:10.1016/S0169-555X(98)00089-0.
802 Harvey, A.M., 2002. The role of base-level change on the dissection of alluvial fans: case
803 studies from southeast Spain and Nevada. Geomorphology 45, 67-87. doi:
804 10.1016/S0169-555X(01)00190-8.
805 Harvey, A.M., 2005. Differential effects of base level, tectonic setting, and climatic change on
806 Quaternary alluvial fans in the northern Great Basin, Nevada, USA. In: Harvey, A.M.,
807 Mather, A.E., Stokes, M. (Eds.), Alluvial Fans. London Geological Society, London, pp.
808 117-131.
809 Harvey, 2011. Dryland Alluvial Fans. In: Thomas, D.S.G. (Ed.), Arid Zone Geomorphology:
810 Process, Form and Change in Drylands. John Wiley, Chichester, pp. 333-371.
811 Harvey, A.M., Wigand, P.E., Wells, S.G., 1999. Response of alluvial fan systems to the late
812 Pleistocene to Holocene climatic transition: Contrasts between the margins of pluvial
813 Lakes Lahontan and Mojave, Nevada and California, USA. Catena 36, 255–281.
814 doi:10.1016/S0341-8162(99)00049-1.
815 Hetzel, R., Niedermann, S., Ivy-Ochs, S., Kubik, P.W., Tao, M., 2002. ^{21}Ne versus ^{10}Be and
816 ^{26} Al exposure ages of fluvial terraces : the influence of crustal Ne in quartz. Earth and
817 Planetary Science Letters 201, 575-591. doi:10.1016/S0012-821X(02)00748-3.
818 Heyman, J., 2014. Paleoglaciation of the Tibetan Plateau and surrounding mountains based on
819 exposure ages and ELA depression estimates. Quaternary Science Reviews 91, 30-41.
820 doi:10.1016/j.quascirev.2014.03.018.
821 Hooke, R.LeB., 1967. Processes on arid region alluvial fans. Journal of Geology 75, 438-460.
822 doi: 10.1086/627271.

Hooke, R.LeB., 1972. Geomorphic evidence for late-Wisconsin and Holocene tectonic deformation, Death Valley, California. Geol. Soc. Am. Bull. 83, 2073-2098. doi: 10.1130/0016-7606(1972)83[2073:GEFLAH]2.0.CO;2.

Hooke, R.LeB., Dorn, R.I., 1992. Segmentation of alluvial fans in Death Valley, California—new insights from surface-exposure dating and laboratory modeling. Earth Surface Processes and Landforms 17, 57–574. doi: 10.1002/esp.3290170603.

Hunt, C.B., Mabey, D.R., 1966. Stratigraphy and structure, Death Valley, California. U.S. Geological Survey Professional Paper 494-A, 162 pp.

Ivy-Ochs, S., 1996. The dating of rock surfaces using in situ produced 10Be, 26Al, and 36Cl, with examples from Antarctica and the Swiss Alps. Ph.D. Thesis, Swiss Federal Institute of Technology, Zürich, 196 pp.

Jannick, N.O., Phillips, F.M., Smith, G.I., Elmore, D., 1991. A 36Cl chronology of lacustrine sedimentation in the Pleistocene Owens River system. Geological Society of America Bulletin 103, 1146-1159. doi: 10.1130/0016-7606(1991)103<1146:ACCOLS>2.3.CO;2.

Jennings, C.W., Burnett, J.L., Troxel, B.W., 1962. Geologic map of the Trona sheet, California. Scale 1:250000. California Division of Mines and Geology.

Johnson, B.K., 1957. Geology of a part of the Manly Peak quadrangle, southern Panamint range, California. University of California Publications in the Geological Sciences 30, 353-423.

Kim, W., Jerolmack, D.J., 2007. The pulse of calm fan deltas. Journal of Geology 116, 315-330. doi: 10.1086/588830.

Klinger, R.E., 2001. Road log for day A, northern Death Valley. In: Machette, M.N., Johnson, M.L., Slate, J.L. (Eds.), Quaternary and late Pliocene geology of the Death Valley region: Recent observations on tectonics, stratigraphy, and lake cycles (Guidebook for the 2001 Pacific Cell— Friends of the Pleistocene Field Trip, Denver, Colorado), U.S. Geological Survey Open File Report 01-51, pp. 6–20.

Klinger, R.E., Piety, L.A., 2001, Holocene faulting and slip rates along the Black Mountains fault zone near Mormon Point, In: Machette, M.N., Johnson, M.L., Slate, J.L. (Eds.), Quaternary and late Pliocene geology of the Death Valley region: Recent observations on tectonics, stratigraphy, and lake cycles (Guidebook for the 2001 Pacific Cell—Friends of the Pleistocene Field Trip, Denver, Colorado), U.S. Geological Survey Open File Report 01-51, pp. 193–203.

Knott, J.R., Wells, S.G., 2001. Late Pleistocene slip rate of the Black Mountains fault zone, In: Machette, M.N., Johnson, M.L., Slate, J.L. (Eds.), Quaternary and Late Pliocene Geology of the Death Valley Region: Recent Observations on Tectonics, Stratigraphy, and Lake Cycles (Guidebook for the 2001 Pacific Cell, Friends of the Pleistocene Field Trip, Denver, Colorado), U.S. Geological Survey Open File Report 01-51, pp. 103–104.

Knott, J.R., Tinsley, J.C., Wells, S.G., 2002. Are the benches at Mormon Point, Death Valley, California, USA, scarps or strandlines? Quaternary Research 58, 352–360. doi: 10.1006/qres.2002.2382.

Knott, J.R., Sarna-Wojcicki, A.M., Machette, M.N., Klinger, R.E., 2005. Upper Neogene stratigraphy and tectonics of Death Valley – a review. Earth Science Reviews 73, 245-270. doi: 10.1016/j.earthscirev.2005.07.004.

Kohl, C.P., Nishiizumi, K., 1992. Chemical isolation of quartz for measurement of in-situ-produced cosmogenic nuclides. Geochimica et Cosmochimica Acta 56, 3583–3587. doi:10.1016/0016-7037(92)90401-4.

Korschinek, G., Bergmaier, A., Faestermann, T., Gerstmann, U.C., Knie, K., Rugel., G., Wallner, A., Dillmann, I., Dollinger, G., von Gostomski, C.L., Kossert, K., Maiti, M., Poutivtsev, M., Remmert, A., 2010. A new value for the half-life of 10Be by heavy ion elastic recoil detection and liquid scintillation counting. Nuclear Instruments and Methods in Physics Research B 268, 187-191.

Ku, T.-L., Luo, S., Lowenstein, T.K., Li, J., Spencer, R.J., 1998. U-series chronology of

875 lacustrine deposits in Death Valley, California. Quaternary Research 50, 261–275.
876 doi:10.1006/qres.1998.1995.
877 Kubik, P.W., Christl, M., 2010. ^{10}Be and ^{26}Al measurements at the Zurich 6 MV Tandem
878 facility. Nuclear Instruments and Methods in Physics Research B 268, 880-883.
879 Lal, D., 1991. Cosmic ray labeling of erosion surfaces: in situ nuclide production rates and
880 erosion models. Earth and Planetary Science Letters 104, 424–439. doi:10.1016/0012-
881 821X(91)90220-C.
882 Le, K., Lee, J., Owen, L., Finkel, R., 2007. Late Quaternary slip rates along the Sierra Nevada
883 frontal fault zone, California: Slip partitioning across the western margin of the Eastern
884 California Shear Zone- Basin and Range Province. Geological Society of America
885 Bulletin 119. doi: 10.1130/B25960.1.
886 Li, H.C., Lowenstein, T.K., Brown, C.N., Ku, T.L., Luo, S.D., 1996. A 100 ka record of water
887 tables and paleoclimates from salt cores, Death Valley, California. Palaeogeography,
888 Palaeoclimatology, Palaeoecology 123, 179-203. doi: 10.1016/0031-0182(95)00123-9.
889 Liu, T, Broecker, W.S., 2008. Rock varnish microlamination dating of late Quaternary
890 geomorphic features in the drylands of western USA. Geomorphology 93, 501-523.
891 Doi:10.1016/j.geomorph.2007.03.015.
892 Lowenstein, T.K., Li, J., Brown, C., Roberts, S.M., Ku, T.L., Luo, S., Yang, W., 1999. 200
893 k.y. paleoclimate record from Death Valley salt core. Geology 27, 3–6.
894 doi:10.1130/0091-7613(1999)027<0003:KYPRFD>2.3.CO;2.
895 Machette, M.N., Johnson, M.L., Slate, J.L. 2001. Quaternary and Late Pliocene Geology of
896 the Death Valley Region: Recent Observations on Tectonics, Stratigraphy, and Lake
897 Cycles (Guidebook for the 2001 Pacific Cell – Friends of the Pleistocene Fieldtrip). U.S.
898 Geological Survey Open-File Report 2001-51, pp. 246.
899 Machette, M.N., Crone, A.J., 2001. Late Holocene faulting on the Old Ghost alluvial-fan
900 complex. In: Machette, M.N., Johnson, M.L., Slate, J.L. (Eds.), Quaternary and Late

Pliocene Geology of the Death Valley Region: Recent Observations on Tectonics, Stratigraphy, and Lake Cycles (Guidebook for the 2001 Pacific Cell – Friends of the Pleistocene Fieldtrip). U.S. Geological Survey Open-File Report 2001-51, pp. 67-69.

Machette, M.N., Slate, J.L., Phillips, F.M., 2008. Terrestrial Cosmogenic-Nuclide Dating of Alluvial Fans in Death Valley, California. U.S. Geological Survey Professional Paper 1755, 54 pp.

Marchetti, D.W., Cerling, T.E., 2005. Cosmogenic ^{3}He exposure ages of Pleistocene debris flows and desert pavements in Capitol Reef National Park, Utah. Geomorphology 67, 423–435. doi:10.1016/j.geomorph.2004.11.004.

Matmon, A., Schwartz, D.P., Finkel, R., Clemmens, S., Hanks, T., 2005. Dating offset fans along the Mojave section of the San Andreas fault using cosmogenic Al26 and Be10. Geological Society of America Bulletin 117, 795-807. doi: 10.1130/B25590.1.

Matmon, A., Nichols, K., Finkel, R., 2006. Isotopic insights into smoothening of abandoned fan surfaces, Southern California. Quaternary Research 66, 109–118. doi:10.1016/j.yqres.2006.02.010.

Menges, C.M., Taylor, E.M., Workman, J.B., Jayko, A.S., 2001. Regional surficial-deposit mapping in the Death Valley area of California and Nevada in support of ground-water modeling. In: Machette, M.N., Johnson, M.L., Slate, J.L. (Eds.), Quaternary and Late Pliocene Geology of the Death Valley Region: Recent Observations on Tectonics, Stratigraphy, and Lake Cycles (Guidebook for the 2001 Pacific Cell, Friends of the Pleistocene Field Trip, Denver, Colorado). U.S. Geological Survey Open File Report 01-51, pp. 151-166.

Miller, J.M.G., 1985. Geologic map of a portion of the Manly Peak quadrangle, southern Panamint mountains, California. California Division of Mines and Geology Open-File Report 85-9.

926 Nicholas, A.P., Quine, T.A., 2007. Modeling alluvial landform chane in the absence of
927 external environmental forcing. Geology 35, 527-530. doi: 10.1130/G23377A.
928 Nishiizumi, K., 2004. Preparation of ^{26}Al AMS standards. Nuclear Instruments and Methods
929 in Physics Research B 223-224, 388-392.
930 Nishiizumi, K., Kohl, C.P., Arnold, J.R., Klein, J., Fink, D., Middleton, R., 1993. Role of in
931 situ cosmogenic nuclides ^{10}Be and ^{26}Al in the study of diverse geomorphic processes.
932 Earth Surface Processes and Landforms 18, 407-425. doi: 10.1002/esp.3290180504.
933 Ochs, M., Ivy-Ochs, S., 1997. The chemical behavior of Be, Al, Fe, Ca and Mg during AMS
934 target preparation from terrestrial silicates modeled with chemical speciation
935 calculations. Nuclear Instruments and Methods in Physics Research B 123, 235–240.
936 doi:10.1016/S0168-583X(96)00680-5.
937 Owen, L.A., Frankel, K.L., Knott, J.R., Reynhout, S., Finkel, R.C., Dolan, J.F., Lee, J., 2011.
938 Beryllium-10 terrestrial cosmogenic nuclide surface exposure dating of Quaternary
939 landforms in Death Valley. Geomorphology 125, 541–557.
940 doi:10.1016/j.geomorph.2010.10.024.
941 Owen, L. a., Clemmens, S.J., Finkel, R.C., Gray, H., 2014. Late Quaternary alluvial fans at
942 the eastern end of the San Bernardino Mountains, Southern California. Quaternary
943 Science Reviews 87, 114–134. doi:10.1016/j.quascirev.2014.01.003.
944 Reheis, M.C., Slate, J.L., Throckmorton, C.K., McGeehin, J.P., Sarna-Wojcicki, a M.,
945 Dengler, L., 1996. Late Quaternary sedimentation on the Leidy Creek fan, Nevada-
946 California: geomorphic responses to climate change. Basin Research 8, 279–299.
947 doi:10.1046/j.1365-2117.1996.00205.x.
948 Regmi, N.R., McDonald, E.V., Bacon, S.N., 2014. Mapping Quaternary alluvial fans in the
949 southwestern United States based on multiparameter surface roughness of lidar
950 topographic data. Journal of Geophysical Research – Earth Surface 119, 12-27. doi:
951 10.1001/2012JF002711.

952 Repka, J.L., Anderson, R.S., Finkel, R.C., 1997. Cosmogenic dating of fluvial terraces,
953 Fremont River, Utah. Earth and Planetary Science Letters 152, 59–73.
954 doi:10.1016/S0012-821X(97)00149-0.
955 Ritter, J.B., Miller, J.R., Enzel, Y. et al., 1993. Quaternary evolution of Cedar Creek Alluvial
956 Fan, Montana. Geomorphology 8, 287-304. doi:10.1016/0169-555X(93)90025-W.
957 Ritter, J.B., Miller, J.R., Husek-Wulforst, J., 2000. Environmental controls on the evolution of
958 alluvial fans in Buena Vista Valley, north central Nevada, during the late Quaternary
959 time. Geomorphology 36, 63-87. doi: 10.1016/S0169-555X(00)00048-9.
960 Schürch, P., Densmore, A.L., Ivy-Ochs, S., Rosser, N.J., KOber, F., Schlunegger, F.,
961 McArdell, B., Alfimov, V., 2016. Quantitative reconstruction of late Holocene surface
962 evolution on an alpine debris flow fan. Geomorphology 275, 46-57. doi:
963 10.1016/j.geomorph.2016.09.020.
964 Smith, G.I., 1984. Paleohydrologic regimes in the Southwestern Great Basin, 0-3.2 my ago,
965 compared with other long records of ‘global’ climate. Quaternary Research 22, 1–17.
966 doi: 10.1016/0033-5894(84)90002-4.
967 Smith, G.I., Bischoff, J.L., 1997. An 800,000-year paleoclimatic record from core OL-92,
968 Owens Lake, Southeast California. Geological Society of America Special Paper 317,
969 165 pp.
970 Sohn, M.F., Mahan, S.A., Knott, J.R., Bowman, D.D., 2007. Luminescence ages for alluvial-
971 fan deposits in Southern Death Valley: Implications for climate-driven sedimentation
972 along a tectonically active mountain front. Quaternary International 166, 49-60. doi:
973 10.1016/j.quaint.2007.01.002.
974 Sohn, M.F., Knott, J.R., Mahan, S.A., 2014. Paleoseismology of the Southern Section of the
975 Black Mountains and Southern Death Valley Fault Zones, Death Valley, United States.
976 Environmental and Engineering Geoscience 10, 177-198. doi:
977 10.2113/gseegeosci.20.2.177.

978 Spelz, R.M., Fletcher, J.M., Owen, L.A., Caffee, M.W., 2008. Quaternary alluvial-fan
979 development, climate and morphologic dating of fault scarps in Laguna Salada, Baja
980 California, Mexico. Geomorphology 102, 578-594. doi:
981 10.1016/j.geomorph.2008.06.001.
982 Stone, J.O., 2000. Air pressure and cosmogenic isotope production, JGR-Solid Earth 105,
983 23753-23759. doi: 10.1029/2000JB900181.
984 Suwa, H., Okuda, S., 1983. Deposition of debris flows on a fan surface, Mt. Yakedake, Japan.
985 Zeitschrift für Geomorphologie N.F. Supplement Bd 46, 79-101.
986 Ventra, D., Nichols, G.J., 2014. Autogenic dynamics of alluvial fans in endorheic basins:
987 outcrop examples and stratigraphi significance. Sedimentology 56, 1569-1589.
988 doi:10.1111/sed.12077.
989 Wells, S.G., McFadden, L.D., Dohrenwend, J.C., 1987. Influence of late Quaternary climatic
990 changes on geomorphic and pedogenic processes on a desert piedmont, Eastern Mojave
991 Desert, California. Quaternary Research 27, 130–146. doi:10.1016/0033-5894(87)90072-
992 X.
993 Whipple, K.X., Trayler, C.R., 1996. Tectonic control of fan size: the importance of spatially
994 variable subsidence rates. Basin Research 8, 351-366. doi: 10.1046/j.1365-
995 2117.1996.00129.x.
996 Whipple, K.X., Dunne, T., 1992. The influence of debris-flow rheology on fan morphology,
997 Owens Valley, California. Geological Society of America Bulletin 104, 887-900. doi:
998 10.1130/0016-7606(1992)104<0887:TIODFR>2.3.CO;2.
999 Winograd, I.J., Szabo, B.J., Coplen, T.B., Riggs, A.C., Kolesar, P.T., 1985. Two-million-year
1000 record of deuterium depletion in Great Basin groundwaters. Science 227, 519–522. doi:
1001 10.1126/science.227.4686.519.
1002 Wolkowinsky, A.J., Granger, D.E., 2004. Early Pleistocene incision of the San Juan River,
1003 Utah, dated with ^{26}Al and ^{10}Be. Geology 32, 749-752. doi: 10.1130/G20541.1.

Zehfuss, P.H., Bierman, P.R., Gillespie, A.R., Burke, R.M., Caffee, M.W., 2001. Slip rates on the fish springs fault, Owens Valley, California, deduced from cosmogenic ^{10}Be and ^{26}Al and soil development on fan surfaces. Bull. Geol. Soc. Am. 113, 241–255. doi:10.1130/0016-7606(2001)113<0241:SROTFS>2.0.CO;2.

10. Figure Captions

Figure 1:

Shaded-relief map of the study location showing the Panamint Range and Death Valley, California. Topographic data are based on USGS 10 m National Elevation Data. The white box indicates the location of Fig. 2 and 4. Note the difference in surface texture on the Warm Springs fan compared to all other fans on the west side of Death Valley. BMFZ, Black Mountain Fault Zone.

Figure 2:

Shaded-relief map of the Warm Springs fan showing the textural fan surface characteristics. Topography is derived from Airborne Laser Swath Mapping (ALSM) topographic data with resolution of 1 m/pixel. Solid lines labeled with letters indicate the location of the topographic profiles shown in Fig. 5. The original boundaries of fan units mapped by Hunt and Maybe (1966) are indicated by labels Qg2, Qg3, and Qg4. Dashed lines delineate fault offsets on the fan (for clarity only selected offsets are shown); dotted line indicates the 65 m a.s.l. contour line, where a paleoshoreline cut into fan deposits on the Warm Springs fan. X-Y coordinates are in UTM projection (zone 11).

Figure 3:

Field photos of fan surfaces on the Warm Springs fan. A, overview over the fan surfaces of unit Qg2 showing the planar surfaces with darkly varnished desert pavement. View is to the north/northeast. B, fan surface Qg2 at sampling location 10303_1 (~925 ka). View is to the south/southeast. C, example for well-developed desert pavement with darkly varnished clasts at sampling location 10303_1. D, Surface characteristics in the active channel (Qg4) with well-preserved channel-levee morphology. View is to the west/northwest.

Figure 4:

Relative and absolute chronology of fan units on the Warm Springs fan. Colored fan surfaces represent the relative chronology based on geomorphological criteria such as surface dissection and pavement development. Note that the boundary of our Qg2 is similar to Hunt and Maybe's original map (1966) while unit Qg3 differs significantly from the original map (see Fig. 2 for comparison). Red dots show sample locations for cosmogenic ^{10}Be surface exposure dating. See Tables 2 and 3 for sample details. X-Y coordinates are in UTM projection (zone 11).

Figure 5:

Topographic profiles across the Warm Springs fan surfaces showing the long-wavelength relief of the fan surfaces. Note the differences in incision depths on fan units Qg4 to Qg2. Topographic data were extracted from 1 m-resolution Airborne Laser Swath Mapping data. For the profile locations see Fig. 2.

Figure 6:

Box-and-whisker plots of ^{10}Be ages plotted for surface units Qg2, Qg3, and Qg4. The box encloses the area between the first and third quartiles and the horizontal line represents the median. Whiskers show one standard deviation. Sample point outside box Qg2 lies one standard deviation outside from the mean.

Figure 7:

Plot of ^{10}Be concentrations from incised channel samples vs distance from the catchment outlet. The minimum inherited component at the catchment outlet makes about 10-20% of the measured ages on surface unit Qg2, which is within the error of our ages. The significantly

higher inherited concentrations at the distal fan overlap or even exceed measured concentrations on the fan unit Qg3. This implies that we cannot provide reliable estimates on the timing fan surface abandonment. Note the plotted concentration from surface samples for comparison.

Figure 8:

Plot of $^{26}Al/^{10}Be$ vs ^{10}Be (see explanation of plot in text). All measured sample concentrations are normalized to sea level after Stone (2000).

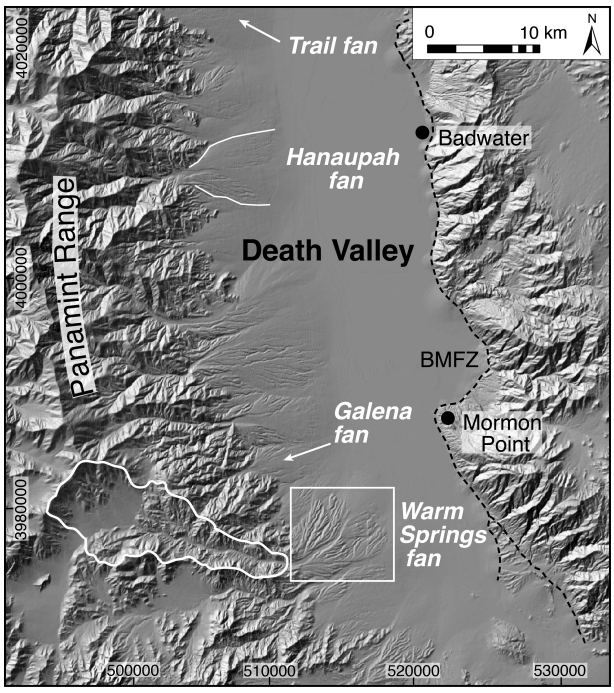

Figure 1

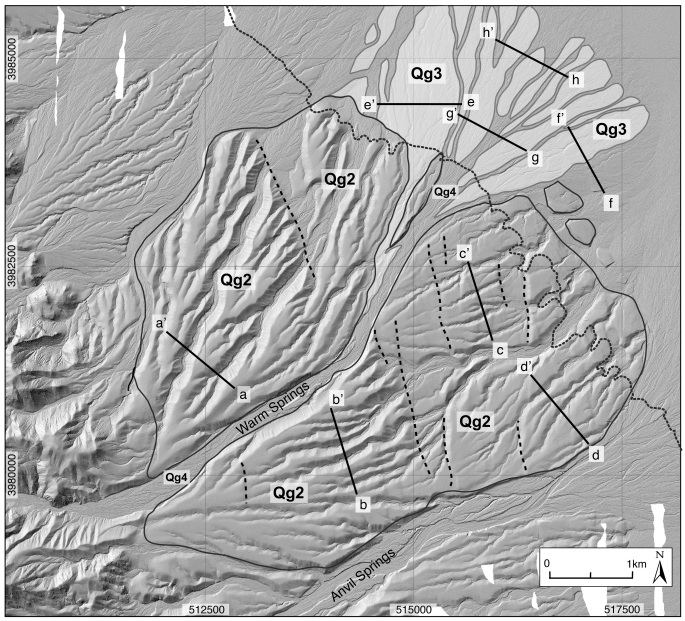

Figure 2

Figure 3

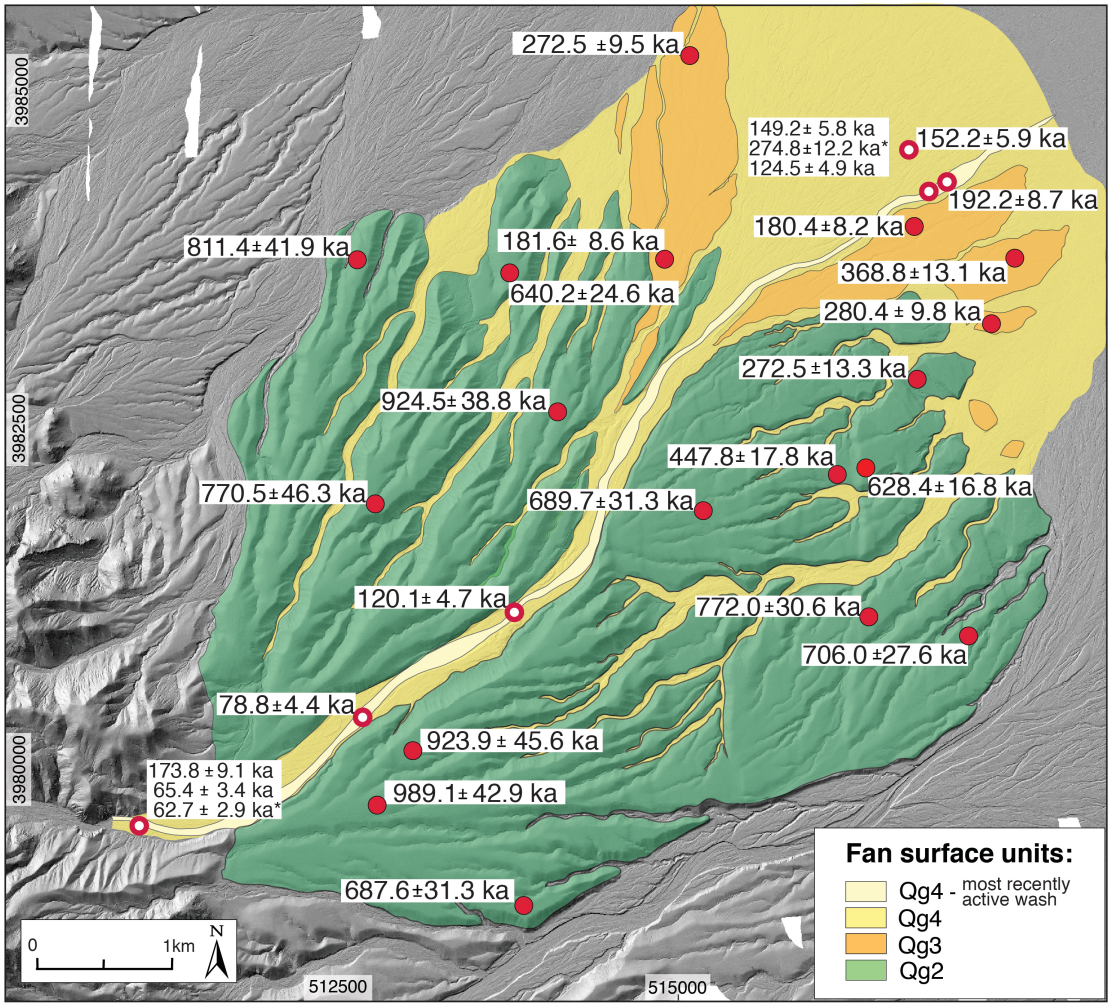
272.5 ±9.5 ka
149.2± 5.8 ka
274.8±12.2 ka*
124.5± 4.9 ka
152.2±5.9 ka
192.2±8.7 ka
180.4±8.2 ka
811.4±41.9 ka
181.6± 8.6 ka
640.2±24.6 ka
368.8±13.1 ka
280.4 ± 9.8 ka
272.5±13.3 ka
924.5± 38.8 ka
447.8±17.8 ka
628.4±16.8 ka
770.5±46.3 ka
689.7±31.3 ka
120.1± 4.7 ka
772.0±30.6 ka
706.0 ±27.6 ka
78.8±4.4 ka
923.9 ± 45.6 ka
173.8 ±9.1 ka
65.4 ± 3.4 ka
62.7 ± 2.9 ka*
989.1± 42.9 ka
687.6±31.3 ka
3985000
3982500
3980000
0
1km
N
512500
515000
Fan surface units:
Qg4 - most recently active wash
Qg4
Qg3
Qg2

Figure 4

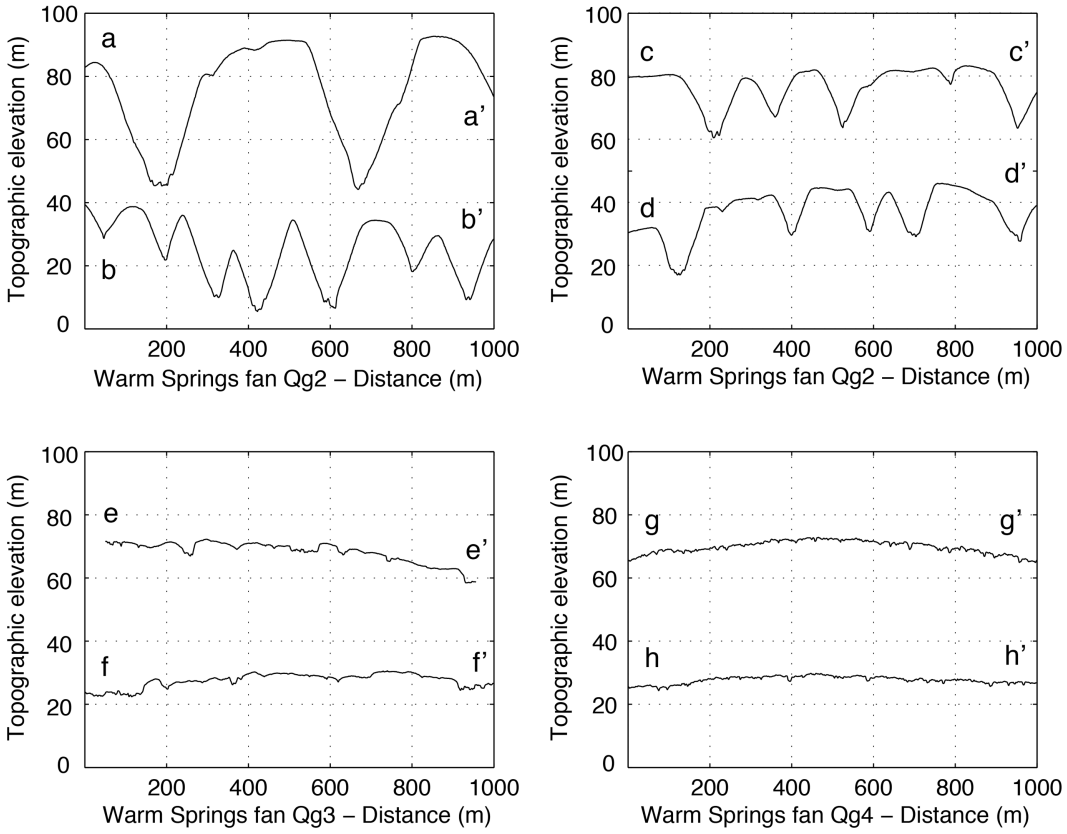

Figure 5

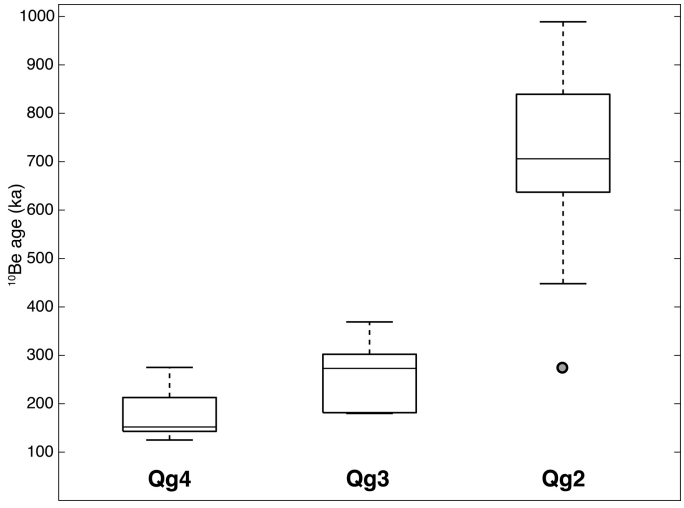

Figure 6

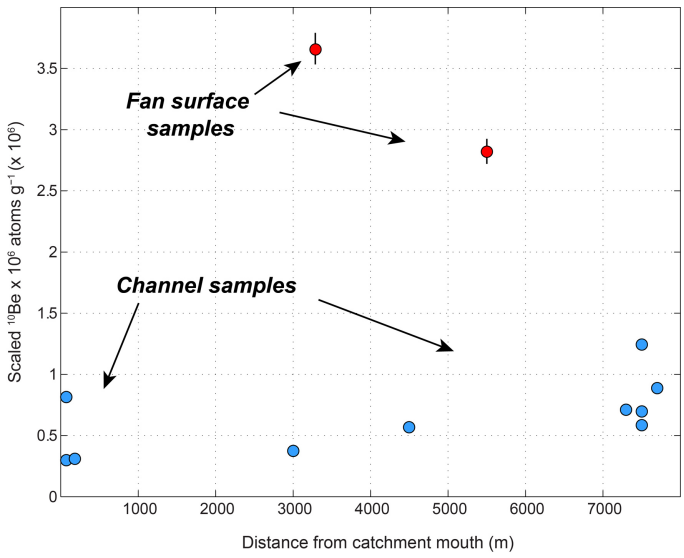

Figure 7

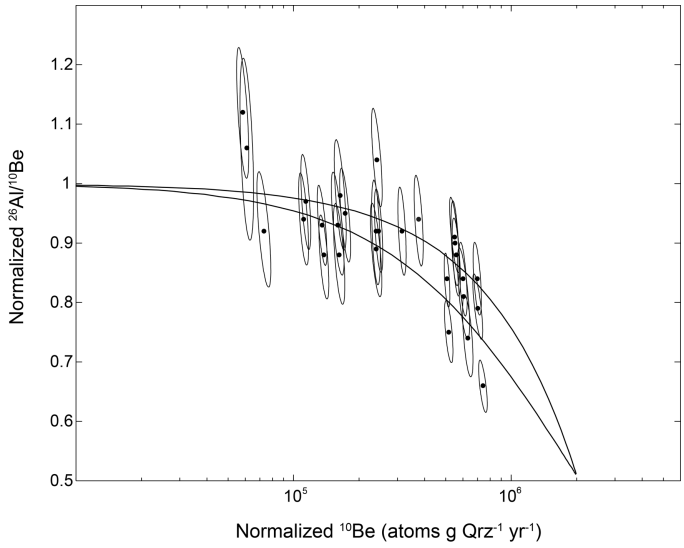

Figure 8